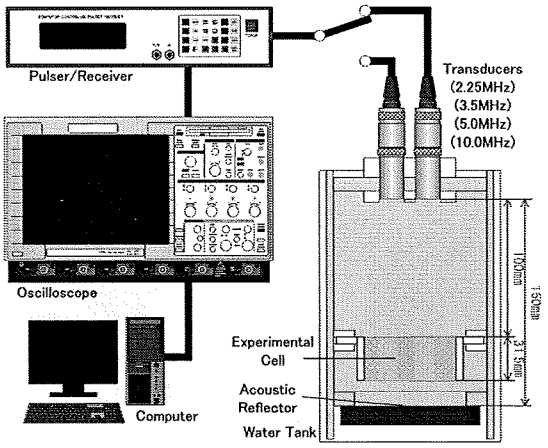

Figure 4. Schematic of the experimental apparatus.

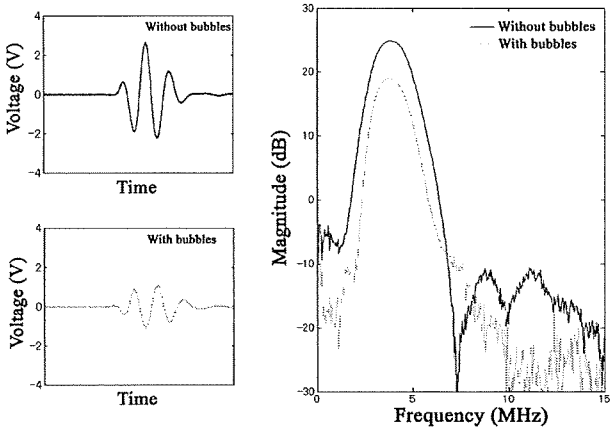

Figure 5. An example of received pulses and their power spectra measured with 3.5 MHz transducer. The left diagrams show received pulses passed through the cell twice: The upper and lower figures shows received pulses without and with lipid bubbles, respectively. The right diagram shows their power spectra, without and with lipid bubbles in the experimental cell.

RESULTS

First, we measured power spectra both with and without lipid bubbles, and calculated the attenuation spectrum, which is defined as the division of the difference between them by the total sound path length through the experimental cell, with both acoustic energy and the path length of the experimental call fixed as 100 μJ and 31.5 mm, respectively. The attenuation spectrum, which is used as the index of the difference of the acoustic characteristics between with and without lipid bubbles, is shown in Figure 6 in the case of the lipid bubble solution concentration of 1333 ppm.

Figure 6 is a typical example of the attenuation spectrum. It should be emphasized that, in this frequency range (0-15 MHz), this attenuation spectrum has two peaks. The larger attenuation is observed around the frequency of 1.4 MHz, the other is observed around the frequency of 11.5 MHz. It is understood that the existence of these peaks in the attenuation spectrum is due to the acoustic energy absorption by the lipid bubbles with resonant oscillations; hence the resonant frequencies of the solution of lipid bubbles are evaluated as approximately around the frequencies of 1.4 MHz and 11.5 MHz. These two peaks should be closely related with the distribution characteristics of the lipid bubble diameter, as already shown in Figure 2. Thereafter, these two peaks of the attenuation spectrum are discussed in the context of the acoustic characteristics of the lipid bubbles.

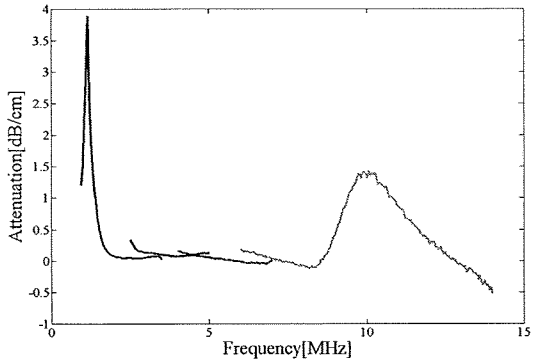

Figure 6. Acoustic attenuation spectra: with acoustic energy of 100 μJ, cell thickness of 31.5 mm, concentration of 1333 ppm.

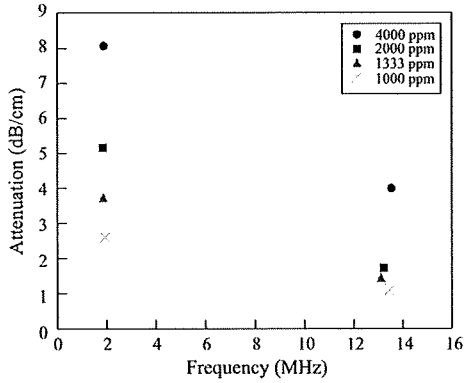

Figure 7. Peak attenuation with acoustic energy of 100 μJ, cell thickness is 31.5 mm, concentrations of 1000 ppm, 1333 ppm, 2000 ppm, and 4000 ppm.

Figure 7 shows the effects of concentration of the lipid bubble solution on the magnitudes of the attenuation at the two peaks of the attenuation spectrum. Here, the acoustic energy and the length of the experimental cell are fixed as 100 μJ and 31.5 mm, as before. Four types of lipid bubble solutions with the concentration of 1000 ppm, 1333 ppm, 2000 ppm, and 4000 ppm are used. It should be noted that the magnitudes of the attenuation at both of the two peaks decrease with the decrease in the concentration of the lipid bubble solution. The concentration of the solution is proportional to number of lipid bubbles per unit volume, and consequently to the amount of energy absorbed by the resonant frequencies of the lipid bubbles.

In order to discuss the effects of the total sound path length, we compare the attenuation spectra obtained by using two cells with different lengths of 31.5 mm and 15.0 mm, respectively. Figure 8 shows the effects of cell length on the magnitude of the attenuation at the two peaks of the attenuation spectrum, in the case that the acoustic energy is 100 μJ and the concentration of the lipid bubble solution is 2000 ppm. There exist little influences of the difference in the cell length; hence the magnitude of the attenuation peak is independent of the total path length through the lipid bubble solution.

As has been already discussed, the two dominant peaks in the attenuation spectrum obtained by this experiment are related to the resonance of the lipid bubbles. A resonant frequency increases with the decrease in the diameter of bubbles. Therefore, the resonant frequency observed in the vicinity of 1.4 MHz and 11.5 MHz may be contributed by lipid bubbles with diameter of 1.5 μm of 200 nm, respectively. It should be noted that this discussion should be improved by incorporating the multiple bubble effects.

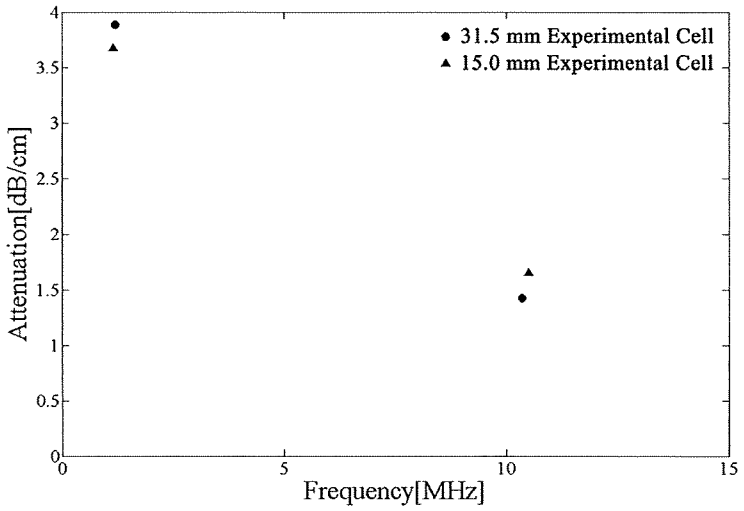

Figure 8. Acoustic attenuation spectra with acoustic energy of 100 μJ concentration of 1333 ppm, cell thickness of 31.5 mm and 15.0 mm.

CONCLUSIONS

We have experimentally studied the resonant frequencies of the lipid bubbles and obtained the following results:

(1) The attenuation spectrum, which is defined as the division of the difference of power spectra between with and without lipid bubbles by the total sound path length through the experimental cell, has two dominant peaks.

(2) The strong attenuations are observed at two different frequencies, around 1.4 MHz and 11.5 MHz, respectively.

(3) The strong attenuation decreases with the decrease in the concentration of the lipid bubble solution.

(4) The strong attenuation is independent of the path length through the lipid bubbles.

ACKNOWLEDGEMENTS

This work was carried out by the aid of Research on Advanced Medical Technology, Ministry of Health, Labor and Welfare (H19-nano-010). The authors would like to express their deepest gratitude towards this grant. Authors would also like to express their gratitude for the help of Hokkaido Innovation through NanoTechnology Support (HINTS, Nanotechnology Network Project Supported by the Ministry of Education, Culture, Sports, Science and Technology).

REFERENCES

1. Suzuki, R., Oda, Y., Namai, E., Takizawa, T., Negishi, Y., Utoguchi, N., Tachibana, K., and Maruyama. K., Development of Site Specific Gene Delivery System with Sonoporation, *J. Pharm. Soc. Jpn.*, Vol. 128, No. 2, pp 187-192, 2008.
2. Maruyama, K., Suzuki, R., Takizawa, T., Utoguchi, N., and Negishi, Y., Drug and Gene Delivery by "Bubble Liposomes" and Ultrasound, *J. Pharm. Soc. Jpn.*, Vol. 127, No. 5, pp 781-787, 2007.
3. Hoff, L, Sontum, P. C., and Hovem, J. M., Oscillations of Polymeric Microbubbles: Effect of the Encapsulating Shell, *J. Acoust. Soc. Am.*, Vol. 107, No. 4, pp 2272-2280, 2000.

A *BTB/POZ* Gene, *NAC-1*, a Tumor Recurrence–Associated Gene, as a Potential Target for Taxol Resistance in Ovarian Cancer

Masako Ishibashi,[1] Kentaro Nakayama,[1] Shamima Yeasmin,[1] Atsuko Katagiri,[1] Kouji Iida,[1] Naomi Nakayama,[1] Manabu Fukumoto,[2] and Kohji Miyazaki[1]

Abstract

Purpose: We previously determined that *NAC-1*, a transcription factor and member of the *BTB/POZ* gene family, is associated with recurrent ovarian carcinomas. In the current study, we investigated further the relationship between NAC-1 expression and ovarian cancer.

Experimental Design: NAC-1 expression was assessed by immunohistochemistry, and clinical variables were collected by retrospective chart review. SiRNA system and *NAC-1* gene transfection were used to asses NAC-1 function in Taxol resistance *in vivo*.

Results: Overexpression of NAC-1 correlated with shorter relapse-free survival in patients with advanced stage (stage III/IV) ovarian carcinoma treated with platinum and taxane chemotherapy. Furthermore, overexpression of NAC-1 in primary tumors predicted recurrence within 6 months after primary cytoreductive surgery followed by standard platinum and taxane chemotherapy. NAC-1 expression levels were measured and compared among the human ovarian cancer cell line (KF28), cisplatin-resistant cell line (KFr13) induced from KF28, and paclitaxel-resistant cell lines (KF28TX and KFr13TX) induced by exposing KF28 and KFr13 to dose-escalating paclitaxel. Overexpression of NAC-1 was observed in only the Taxol-resistant KF28TX and KFr13 TX cells but not in KF28 or cisplatin-resistant KFr13 cells. To confirm that NAC-1 expression was related to Taxol resistance, we used two independent but complementary approaches. *NAC-1* gene knockdown in both KF28TX and KFr13TX rescued paclitaxel sensitivity. Additionally, engineered expression of NAC-1 in RK3E cells induced paclitaxel resistance.

Conclusions: These results suggest that NAC-1 regulates Taxol resistance in ovarian cancer and may provide an effective target for chemotherapeutic intervention in Taxol-resistant tumors.

Ovarian cancer is the most lethal gynecologic malignancy in the world (1). In >70% of cases, the tumor has disseminated beyond the ovaries at the time of diagnosis. In these cases, combined treatment with surgery and chemotherapy is necessary. First-line chemotherapy with platinum drugs and taxanes yields a response rate of >80%; however, nearly all patients relapse. At the time of relapse, ovarian tumors can be rechallenged with platinum drugs and taxanes, with response rates proportional to the disease-free interval after the first treatment. Regardless of the initial response, the long term survival of ovarian cancer patients is still poor, particularly when the cancer is diagnosed at an advanced stage. Patients who relapse, and those who do not initially respond to chemotherapy, are thought to carry hidden drug-resistant cells, which are the cause of tumor relapse and lethality. In ovarian cancer, resistance to chemotherapeutics has been thoroughly studied. A number of mechanisms have been proposed that might be targets of novel chemotherapeutic agents. Many chemotherapeutic drugs induce apoptosis in tumor cells. Therefore, pharmacologic research could be directed at enhancing this process, either by directly activating apoptosis or by lowering the threshold for its initiation by cytotoxic drugs (2).

The genes of the *BTB/POZ* family participate in several cellular functions including proliferation, apoptosis, transcription control, and cell morphology maintenance (3). By serial analysis of gene expression levels in all 130 deduced human *BTB/POZ* genes, we identified *NAC-1* as a carcinoma-associated *BTB/POZ* gene (4), is a transcription repressor, and is involved in self renewal and maintenance of pluripotency in embryonic stem cells (5). NAC-1 is significantly overexpressed in several types of human carcinomas including ovarian serous carcinoma (4). The levels of NAC-1 expression correlate with tumor recurrence in ovarian serous carcinomas and, intense NAC-1 immunoreactivity in primary ovarian tumors predicts early recurrence (4). Additionally, NAC-1 expression is higher in specimens obtained after administration of chemotherapy (6). Finally, overexpression of full-length NAC-1 is sufficient to increase tumorigenecity of ovarian surface epithelial cells and NIH3T3 cells in athymic *nu/nu* mice. Taken together, our previous studies suggest that

Authors' Affiliations: [1]Departments of Obstetrics and Gynecology, Shimane University School of Medicine, and [2]Departments of Pathology, Institute of Development, Aging and Cancer, Tohoku University, Sendai, Japan

Received 9/17/07; revised 1/1/08; accepted 1/13/08.

Grant support: Ministry of Education, Culture, Sports, Science, and Technology in Japan and the Japan Society of Gynecologic Oncology.

The costs of publication of this article were defrayed in part by the payment of page charges. This article must therefore be hereby marked *advertisement* in accordance with 18 U.S.C. Section 1734 solely to indicate this fact.

Requests for reprints: Kentaro Nakayama, Shimane University School of Medicine, Enyacho 89-1, Izumo, Shimane, Japan 6938501. Phone: 81-853-20-2268; Fax: 81-853-20-2264; E-mail: kn88@med.shimane-u.ac.jp.

doi:10.1158/1078-0432.CCR-07-4358

NAC-1 is a tumor recurrence–associated gene with oncogenic potential. The molecular mechanisms underlying these observations are unknown, and how NAC-1 expression contributes to chemotherapy resistance in ovarian cancer is yet to be studied.

The current study examined the role of NAC-1 in ovarian cancer recurrence, investigated the relationship between NAC-1 expression and tumor recurrence, and finally assessed whether NAC-1 is a useful prognostic factor in patients with ovarian cancer.

Materials and Methods

Tissue samples and immunohistochemistry. Paraffin-embedded tumor tissues were obtained from the Department of Obstetrics and Gynecology at the Shimane University Hospital. These included 43 advanced stage (stage III/IV) ovarian carcinomas. Diagnosis was based on conventional morphologic examination of sections stained with H&E staining. Tumors were classified according to the WHO classification. Tumor staging was done according to the International Federation of Gynecology and Obstetrics classification. The clinicopathologic characteristics of the patients included in this study are summarized in Table 1. All patients were primarily treated with cytoreductive surgery, and adjuvant conventional platinum and taxane chemotherapy (Carboplatin AUC5, Paclitaxel 175 mg/m^2, or Docetaxel 70 mg/m^2). All of the cases received at least six cycles of chemotherapy. Acquisition of tissue specimens and clinical information was approved by an institutional review board (Shimane University). The Paraffin tissues were organized into tissue microarrays, which were made by removing 3-mm diameter cores of tumor from each block. The selection of the area to core was made by a surgical pathologist (M. F) and based on review of the H&E slides. NAC-1 mouse monoclonal antibody was a kind gift from Dr. Ie-Ming Shih (Johns Hopkins Medical Institutions, Baltimore, MD). Immunohistochemistry was done on deparaffinized sections using the NAC-1 antibody at a dilution of 1:100 and an EnVision+System peroxidase kit (DAKO). Immunoreactivity was scored by two investigators as follows: 0, undetectable; 1+, weakly positive; 2+, moderately positive; and 3+, intensely positive. NAC-1 immunoreactivity was not detectable (immunointensity score, 0) in normal ovarian epithelium.

Reagent preparation. Paclitaxel and carboplatin were obtained from Bristol-Myers Squib. They were stored at 4°C and were added to the culture medium at several final concentrations.

Quantitative PCR analysis. Of the 43 ovarian cancer samples we examined, 18 were available for gene expression analysis. A total of 24 frozen tissues including 18 cases of ovarian cancer and 6 samples of normal ovary were analyzed for *NAC-1* transcript expression by quantitative real-time PCR using an ABI 7000 (Applied Biosystems) with the SYBR Green dye (Molecular Probes). Detailed procedure of quantitative PCR was described previously (4).

Cell culture and Western blot analysis. The human ovarian carcinoma cell lines KF28, KF28TX, KFr13, and KFr13TX were a kind gift of Dr. Yoshihiro Kikuchi (Ohki Memorial Kikuchi Cancer Clinic for Women, Saitama, Japan; ref. 7). KF28 was the original human ovarian carcinoma–derived cell line, and KF28TX and KFr13 were the Taxol- and cisplatin-resistant lines that were established by repeated exposure of the parent KF28 cells to Taxol and cisplatin, respectively. KFr13TX was the cell line derived from KFr13 cells through exposure to Taxol. All of the cell lines were maintained in DMEM (Life Technologies) supplemented with 10% fetal bovine serum, 100 units/mL of penicillin, and 100 μg/mL of streptomycin. Western blot analysis was done using the same antibody (1:100) on 4 ovarian carcinoma cell lines including KF28, KF28TX, KFr13, and KFr13TX. Detailed procedure of Western blot was described previously (4). Selection of PCMV/*NAC-1* stable clones was done through limiting dilution in selection medium containing 3 ug/mL of Blasticidine (Sigma).

Cell growth inhibition assay. Cytotoxity of Taxol or carboplatin was measured using an 3-(4,5-dimethylthiazol-2-yl)-2,5-diphenyltetrazolium bromide (MTT) colorimetric assay (Sigma Co.). Cells were seeded in 96-well plates at a density of 3,000 cells per well. The cell number was determined indirectly by MTT assay (8). Data were expressed as mean ± 1 SD from triplicates.

Table 1. Clinicopathologic characteristics of patients

A. Association between NAC-1 expression and clinocopathologic factors in patients with advanced stage ovarian cancer

Factors	Patients	NAC-1 immunointensity		*P*
		0+/1+	2+/3+	
FIGO stage				
III	33	15	18	>0.999
IV	10	4	6	
Grade				
G_1	2	0	2	0.495
G_2, G_3	41	19	22	
Histology				
Serous	32	13	19	0.495
Others	11	6	5	
Age (y)				
<60	11	5	6	>0.999
≥60	32	14	18	
Residual tumor				
<1 cm	8	6	2	0.111
≥1 cm	35	13	22	

B. The relationship between NAC-1 expression and recurrence within 6 mo

	No recurrence within 6 mo	Recurrence within 6 mo	*P*
NAC-1 non/low	12 (86%)	2 (14%)	0.0079
NAC-1 high	9 (41%)	13 (59%)	

Abbreviation: FIGO, Federation of Gynecology and Obstetrics.

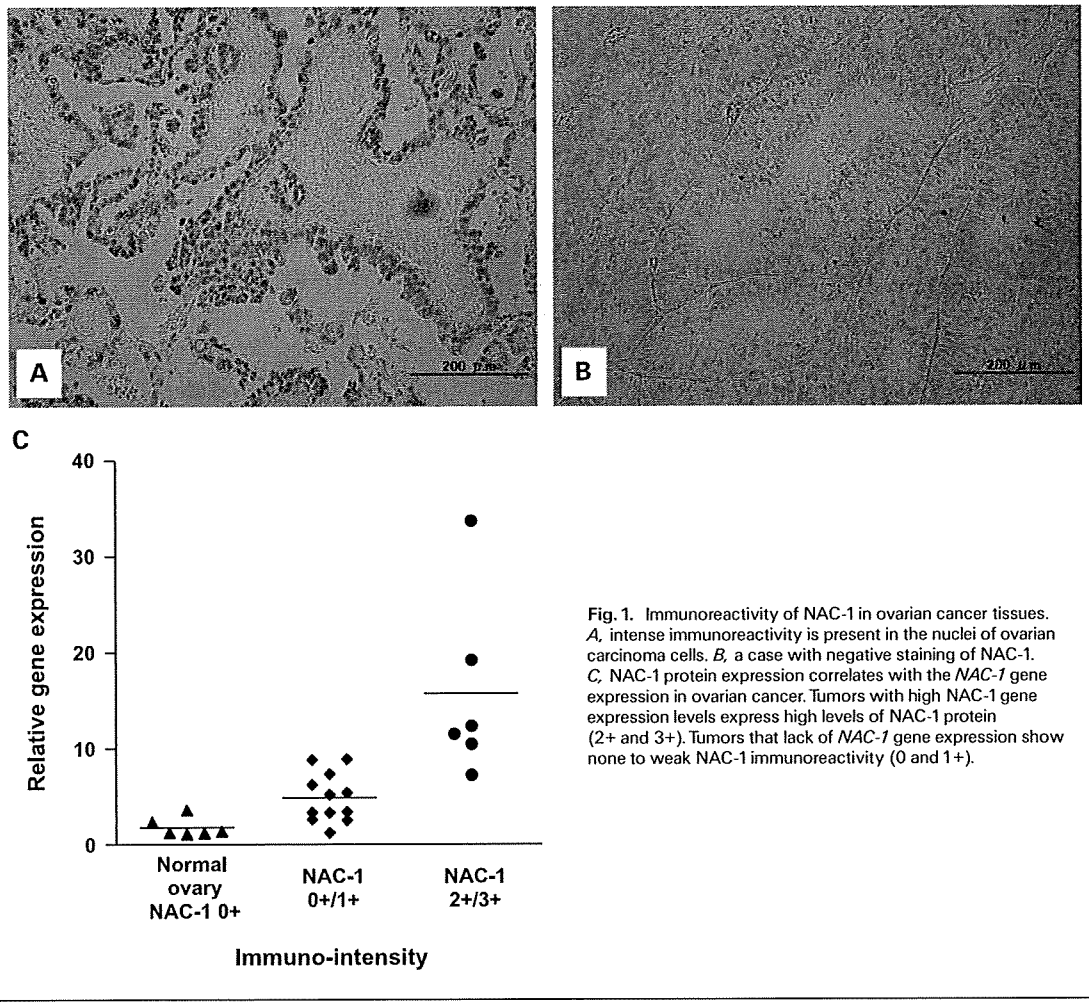

Fig. 1. Immunoreactivity of NAC-1 in ovarian cancer tissues. *A*, intense immunoreactivity is present in the nuclei of ovarian carcinoma cells. *B*, a case with negative staining of NAC-1. *C*, NAC-1 protein expression correlates with the *NAC-1* gene expression in ovarian cancer. Tumors with high NAC-1 gene expression levels express high levels of NAC-1 protein (2+ and 3+). Tumors that lack of *NAC-1* gene expression show none to weak NAC-1 immunoreactivity (0 and 1+).

siRNA knockdown of NAC-1 gene expression. Two siRNAs that targeted *NAC-1* were designed with the following sense sequences: UGAUGUACACGUUGGUGCCUGUCACCA and GAGGAAGAACUCGGUGCCCUUCUCCAU. Control siRNA (luciferase siRNA) was purchased from IDT. Cells were seeded onto 96-well plates and transfected with siRNAs using oligofectamine (Invitrogen). The cell number was determined indirectly by an MTT assay.

Statistical methods for clinical correlation. Relapse-free and overall survivals were calculated from the date of diagnosis to the date of first relapse or last follow up. Age and performance status distributions were similar between patients expressing NAC-1 and those not expressing it. The data were plotted as Kaplan-Meier curves, and the statistical significance was determined by the Log-rank test. Data were censored when patients were lost to follow-up. A Student's *t* test was used to examine the statistical significance in the difference of growth assay data.

Results

Overexpression NAC-1 in advanced stage ovarian carcinoma. In this study, we focused on advanced stage (stage III/IV) ovarian carcinomas because they were the most common. Forty-three stage III or IV primary ovarian carcinoma patients underwent primary cytoreductive surgery that was followed by a standard platinum and taxane chemotherapy regimen. Cytoreduction was optimal in 8 patients (residual tumor, <1 cm) and suboptimal in 35 (residual tumor, ≥1 cm). All of the cases were judged to be in clinical remission after adjuvant conventional chemotherapy. Primary surgical tissues were used for NAC-1 protein immunohistochemistry. Nuclear staining of NAC-1 was observed in some ovarian carcinoma cells (Fig. 1A and B). The immunohistochemistry results are summarized in Table 1. Overexpression of NAC-1 (NAC-1 immunointensity, 2+ and 3+) was observed in 56% (24 of 43) of the analyzed tumors.

Relationship between clinicopathologic findings and NAC-1 expression. Table 1 summarizes the relationship between clinicopathologic findings and overexpression of NAC-1 in ovarian carcinomas. No significant associations were found between NAC-1 overexpression and age, histologic subtype, grade, or status of the residual tumor (Table 1A).

NAC-1 overexpression correlated with shorter relapse-free survival in patients with stage III and IV ovarian carcinoma patients treated with platinum and taxane chemotherapy. Overerexpression of NAC-1 correlated with shorter relapse-free survival in patients with advanced stage (stage III/IV) ovarian carcinoma treated with platinum and taxane chemotherapy.

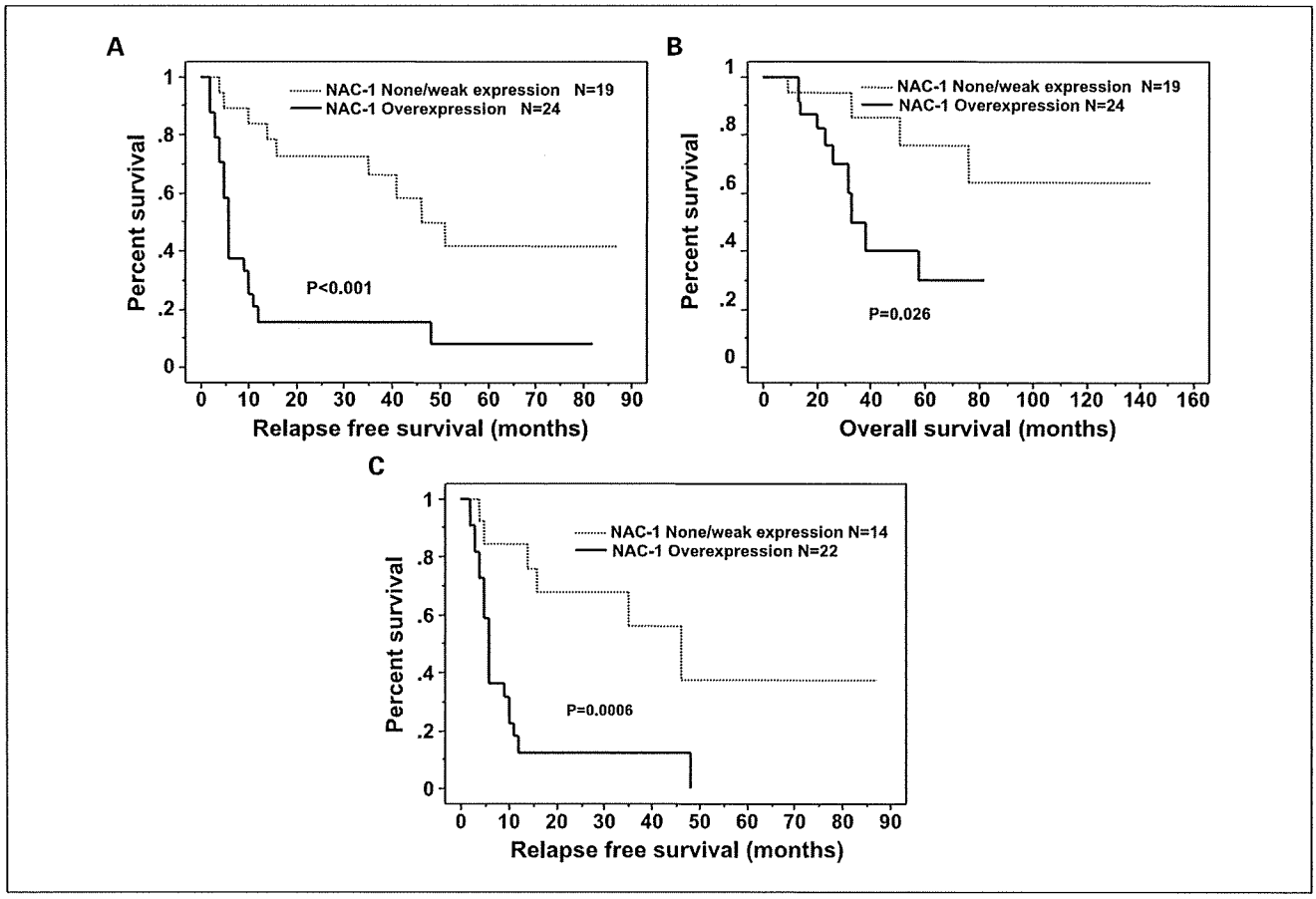

Fig. 2. NAC-1 overexpression correlates with shorter relapse-free survival in patients with stage III/IV ovarian carcinoma who received primary cytoreductive surgery, followed by a standard platinum and taxane chemotherapy regimen. *A*, Kaplan-Meier survival analysis showing that NAC-1 overexpression (*solid line*; $n = 24$) is associated with a shorter relapse-free survival than weak or absent NAC-1 expression in stage III or IV ovarian cancers (*dashed line*; $n = 19$; $P < 0.001$; Log-rank test). *B*, Kaplan-Meier survival analysis showing that NAC-1 overexpression (*solid line*; $n = 24$) is associated with a shorter overall survival than weak or absent NAC-1 expression in stage III or IV ovarian cancers (*dashed line*; $n = 19$; $P = 0.026$; Log-rank test). *B*, Kaplan-Meier survival analysis showing that NAC-1 overexpression (*solid line*; $n = 22$) is associated with a shorter relapse-free survival than weak or absent of NAC-1 expression in stage III or IV ovarian cancer patients who underwent suboptimal primary cytoreduction followed by a standard platinum and taxane chemotherapy regimen (*dashed line*; $n = 14$; $P = 0.024$; Log-rank test).

A total of 43 patients were diagnosed at stage III/IV. Among them, the 24 patients with NAC-1 overexpression had a shorter relapse-free survival compared with those without NAC-1 expression ($P < 0.001$; Log-rank test; Fig. 2A). Univariate analysis showed that both residual tumor (≥1 cm; $P = 0.0039$; Log-rank test) and overexpression of NAC-1 ($P < 0.001$; Log-rank test) were correlated with shorter relapse-free survival. The other clinicopathologic factors including age, histologic subtype, and grade did not influence relapse-free and overall survival (data not shown). A marginally significant correlation between overexpression of NAC-1 and overall survival was found in patients with stage III/IV ovarian carcinomas ($P < 0.026$; Log-rank test; Fig. 2B).

Next, we focused on only the cases with positive residual tumor in advanced stage ovarian carcinoma and evaluated whether overexpression of NAC-1 was still a marker for relapse-free survival in this series of patients. A total of 36 patients with stage III/IV ovarian carcinomas, who underwent suboptimal primary cytoreduction followed by a standard platinum and taxane chemotherapy regimen, were included in the analysis. Among them, the 22 patients with NAC-1 overexpression had a shorter relapse-free survival compared with those without NAC-1 expression ($P = 0.0006$; Log-rank test; Fig. 2C). These findings prompted us to investigate whether NAC-1 overexpression in primary tumors was predictive of the relapse-free interval (the period between when the first-line adjuvant chemotherapy was completed and tumor recurrence) in the 36 patients

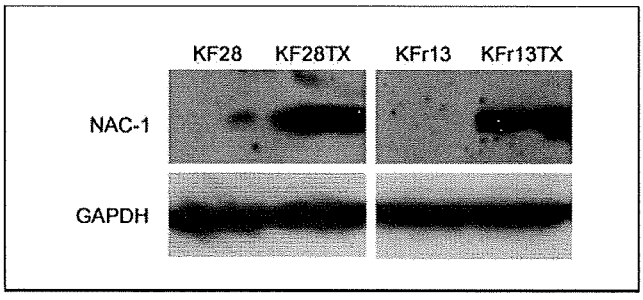

Fig. 3. Western blot analysis of NAC-1 in ovarian cancer cell lines including KF28, KF28TX, KFr13, and KFr13TX. NAC-1 expression is higher in Taxol-resistant KF28TX and KFr13TX cells than in parental KF28 and cisplatin resistant KFr13.

who underwent suboptimal surgery. We found that overexpression of NAC-1 (immunointensity, 2 and 3+) predicted recurrence within 6 months of completing first-line chemotherapy (P = 0.0079; Table 1B).

Correlation of NAC-1 protein expression and NAC-1 *gene expression.* To validate the immunohistochemistry results, we did quantitative real-time PCR to assess the correlation between *NAC-1* gene expression level and NAC-1 immunointensity. *NAC-1* gene expression levels were significantly correlated with higher immunointensity in ovarian carcinomas (Fig. 1C).

NAC-1 expression is higher in Taxol-resistant KF28TX and KFr13TX cells than in parental KF28 and cisplatin-resistant KFr13 cells. To test whether NAC-1 expression was involved in platinum or taxane resistance, we analyzed NAC-1 expression level using platinum or taxane-resistant ovarian cancer cell lines. As previously reported (7), KF28TX and KFr13 cells were derived from KF28 cells based on their resistance to Taxol and cisplatin, respectively. KFr13TX cells were established from KFr13 cells based on their resistance to Taxol. The IC_{50} of Taxol for KF28, KF28TX, KFr13, and KFr13TX were 4.65, 53.30, 2.61, and 12.70 μmol/L, respectively. This indicates that the relative resistances of KF28TX and KFr13TX cells to Taxol are 11.5- and 5.0-fold, respectively, when compared with those of the original KF28 or KFr13 cells. Also, the IC_{50} of cisplatin for KF28, KF28TX, KFr13, and KFr13TX cells were 0.18, 0.14, 0.85, and 0.53 μmol/L, respectively, indicating that the relative resistances of *KFr13* and KFr13TX cells to cisplatin were 4.7 and 2.9 times higher, respectively when compared with those of the original KF28 cells.

Interestingly, when NAC-1 protein levels were examined by Western blotting, expression of NAC-1 was characteristically observed in Taxol-resistant KF28TX and KFr13 TX cells supporting its involvement in Taxol resistance (Fig. 3). In contrast, NAC-1 was not expressed in KFr13 cells derived from KF28 cells through exposure to cisplatin (Fig. 3). NAC-1 protein expression level in KF28TX cells was 1.4-fold higher than that in KFr13TX cells.

Suppression of NAC-1 in Taxol-resistant cell lines KF28TX and KFr13TX and drug resistance to Taxol. *NAC-1* siRNA was transfected into KF28TX and KFr13TX cells, followed by assessment of NAC-1 expression 48 hours later by Western blotting. siRNA treatment significantly reduced NAC-1 protein expression compared with control siRNA treatment (Fig. 4A and B). KF28TX and KFr13TX cells were then transfected with *NAC-1* siRNA or luciferase siRNA as a control and treated with 5 or 1 μmol/L Taxol 48 hours later. Cell growth was then

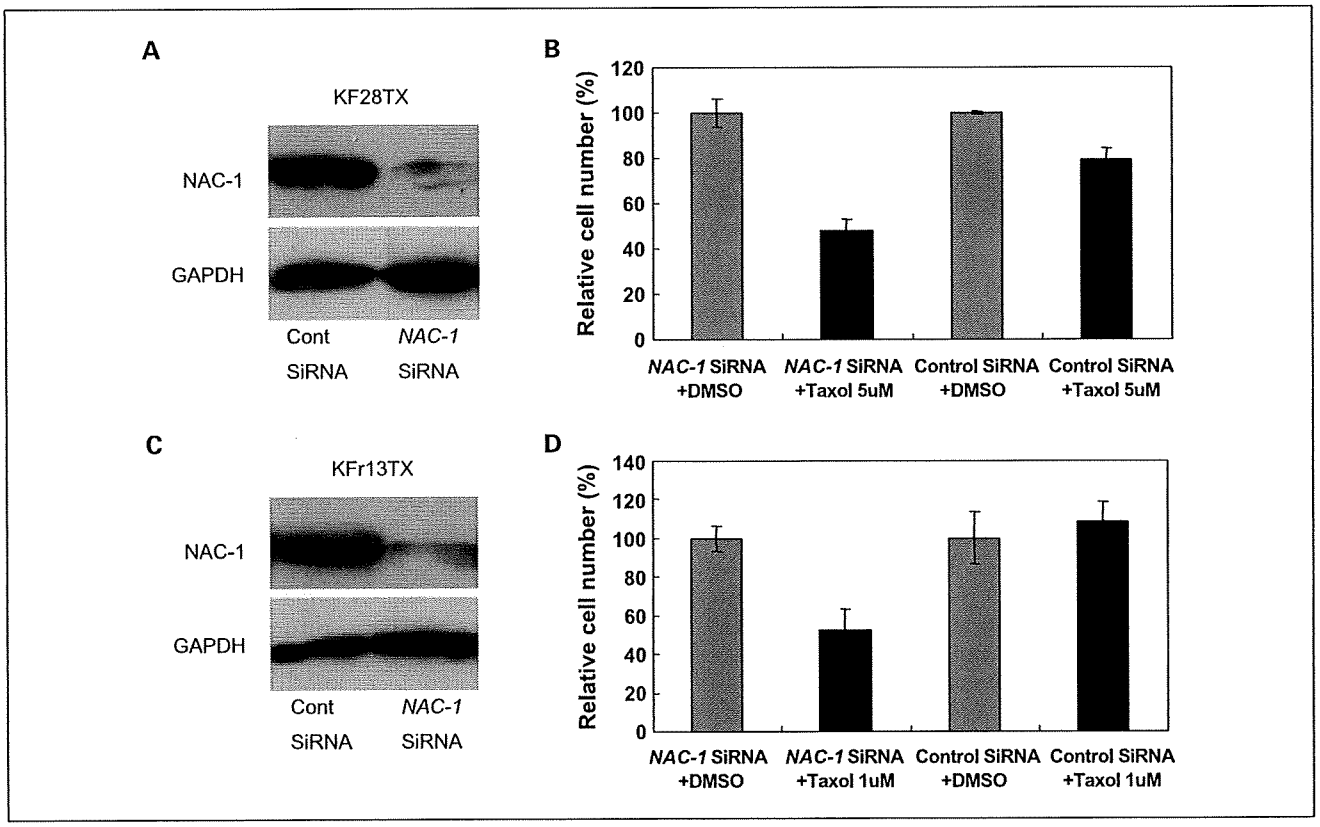

Fig. 4. *A* and *B*, effects of NAC-1 knockdown on Taxol resistance in paclitaxel-resistant KF28TX cells. *A*, Western blot analysis showing a significant reduction of NAC-1 protein in *NAC-1* siRNA – treated cells compared with control SiRNA – treated cells. *B*, KF28TX cells were subsequently transfected with *NAC-1* siRNA or luciferase siRNA as a control and treated with DMSO or 5 μmol/L Taxol 48 h later. Cell growth was then determined with an MTT colorimetric assay after 48 h. There were significantly fewer KF28TX cells after transfection with *NAC-1* siRNA than after transfection with luciferase siRNA ($P < 0.05$). *C* and *D*, effects of NAC-1 knockdown on Taxol resistance in paclitaxel-resistant KFr13TX cells. *C*, Western blot analysis showing a significant reduction of NAC-1 protein in *NAC-1* siRNA – treated cells compared with control SiRNA – treated cells. *D*, KFr13TX cells were transfected with *NAC-1* siRNA or luciferase siRNA as a control and treated with DMSO or 1 μmol/L Taxol 48 h later. Cell growth was then determined with an MTT colorimetric assay after 48 h. There were significantly fewer KFr13TX cells after transfection with *NAC-1* siRNA than after transfection with luciferase siRNA ($P < 0.05$).

determined with an MTT colorimetric assay 48 hours later. We found that there were significantly fewer KF28TX and KFr13TX cells after transfection with *NAC-1* siRNA than after transfection with luciferase siRNA ($P < 0.05$; Fig. 4C and D).

Functional analysis of NAC-1 expression. To confirm that NAC-1 expression was essential for Taxol resistance in cell lines not expressing NAC-1, we used a gene transfection system. We stably expressed the *NAC-1* gene in the normal epithelial cell line RK3E to assess whether expression induced Taxol resistance. Using quantitative real-time PCR, we found that RK3E cells not expressing NAC-1 were sensitive to Taxol. The RK3E cells were then transfected with a vector expressing NAC-1, and three independent clones were randomly selected for functional analysis. Western blot analysis confirmed NAC-1 expression in these clones (Fig. 5A). All of the NAC-1 expressing clones were resistant to Taxol compared with vector-transfected cells (Fig. 5B). There was no difference in sensitivity to carboplatin between vector-transfected cells and the NAC-1-expressing clones (Fig. 5C).

Discussion

The *BTB/POZ* gene family members have assumed a more central role in human cancer in recent years (9–14). Recently, we reported that *NAC-1*, a gene with oncogenic potential was associated with recurrence in ovarian cancer (4). The mechanism by which NAC-1 affects recurrence is, however, unknown.

Our most notable finding was that overexpression of NAC-1 in primary ovarian cancer was highly predictive of a shorter relapse-free interval. To date, there is no molecular marker that predicts the risk of early tumor recurrence. Therefore, NAC-1 expression may have the potential to be used alone or in combination with other markers as a new diagnostic tool to identify ovarian cancer patients with a greater susceptibility to recurrence within 6 months. This is important because at least 60% of advanced-stage ovarian cancer patients who are without clinical evidence of disease after completing primary therapy ultimately develop recurrent disease (15). Recently, Davidoson et al. (6) reported findings similar to ours, showing that NAC-1 expression intensity correlated with shorter progression-free survival in 62 patients with postchemotherapy effusions. Taken together, these observations may have an effect on clinical management. Patients with recurrent ovarian cancer derive the most benefit from secondary cytoreduction if recurrent tumors are small and localized (15–19). Therefore, patients with NAC-1–positive ovarian cancer can be followed more frequently to detect recurrences early enough to benefit from either secondary cytoreductive surgery or second-line chemotherapy.

Next, to elucidate the mechanisms underlying the effects of NAC-1 in ovarian cancer recurrence, we analyzed NAC-1 expression levels in cisplatin or paclitaxel resistance ovarian cancer cell lines (7). Interestingly, overexpression of NAC-1 was characteristically observed in only paclitaxel-resistant KF28TX and KFr13 TX but not in parental KF28 or KFr13 cisplatin–resistant cells.

Because NAC-1 expression was up-regulated in paclitaxel-resistant ovarian cancer cells, we tested the hypothesis that NAC-1 might confer paclitaxel resistance. The *NAC-1* siRNA transfection experiments showed that both KF28TX and KF13rTX paclitaxel–resistant cells became more sensitive to paclitaxel after NAC-1 silencing. This finding suggests that

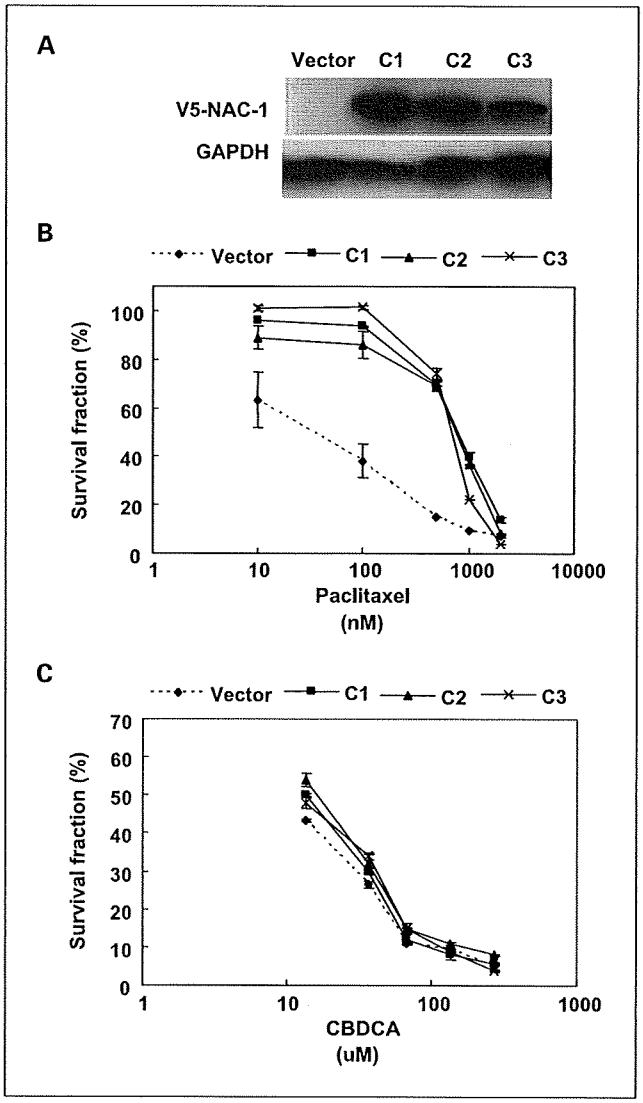

Fig. 5. Functional analysis of NAC-1 expression. *A*, Western blot analysis showing that *NAC-1*–transfected RK3E clones (C1, C2, and C3) express V5-NAC-1 protein. *B*, all of the NAC-1–expressing clones were resistance to Taxol compared with vector-transfected cells. *C*, there was no difference in sensitivity to carboplatin between vector-transfected cells and the NAC-1–expressing clones.

NAC-1 antagonizes the antitumor activity of paclitaxel. Although *NAC-1* silencing by *NAC-1* siRNA rescued paclitaxel sensitivity, it was insufficient to completely restore paclitaxel sensitivity. This is because alterations in genes other than NAC-1, including P-glycoprotein, RhoGDI, and IGFBP-3 mediate paclitaxel resistance in these cell lines (7, 20). A molecular comparison between paclitaxel-sensitive and paclitaxel-resistant human ovarian cancer cell lines identified expression differences in TRAG-3, *β-tubulin*, interleukin 6, interleukin 8, and Raf-1 kinase (21–24). However, alteration in the expression of these genes has not been described in either KF28 or KFr13TX cells (20).

Next, to address whether NAC-1 expression was essential for paclitaxel resistance in cell lines not expressing NCA-1, we used a gene transfection system. All stable RK3E, NAC-1–expressing clones were resistant to paclitaxel but not to carboplatin.

Our studies with siRNA knockdown and gene overexpression established an important role of NAC-1 in Taxol resistance. However, the mechanism for this was unclear. Recently, we reported that NAC-1 controls cell growth and survival by repressing Gadd45GIP1 expression (25). Cross-talk between NAC-1/Gadd45GIP1 pathway and nuclear factor-κB pathway might suppress GADD45 death signals (25). Indeed, inhibition of nuclear factor-κB sensitizes ovarian cancer cells to paclitaxel-induced apoptosis (26, 27). Upon activation, nuclear factor-κB translocates to the nucleus and is associated with c-*myc* up-regulation. This in turn down-regulates Gadd45 proteins (28–30). Gadd45 interacts with Gadd45GIP1 and up-regulates MKK4 through MEKK4/MTK1 activation (31). In this manner, Gadd45 functions as a tumor suppressor (26). The enhanced MKK4 activity activates the proapoptotic c-Jun-NH_2-kinase/p38 signaling, which results in growth arrest and apoptosis (27, 29, 32). Therefore, during tumor development, turning off the Gadd45 pathway seems to be critical for cancer cells to survive in the face of cellular stressors such as paclitaxel. Consequently, NAC-1 may regulate paclitaxel resistance in ovarian cancer by inhibiting Gadd45 cell death signals.

Paclitaxel stabilizes microtubules, causing mitotic arrest, and activates the spindle assembly checkpoint. A key question is how NAC-1 contributes to microtubule-related paclitaxel resistance. We recently reported that knockdown of NAC-1 with a deletion mutant N130-NAC1 dominant-negative protein results in mitotic arrest and leads to apoptosis. This suggests that NAC-1 may interact with *β-tubulin* or regulate mitotic checkpoint genes (4). These observations raise the hypothesis that NAC-1 regulates paclitaxel-related checkpoint genes including *Mad2* and *BubR1* (33).

In summary, we showed that NAC-1, a transcriptional repressor, was associated with tumor recurrence in advanced ovarian cancer. NAC-1 may be a useful marker for predicting recurrence within 6 months of cytoreductive surgery and first-line platinum and taxane-based chemotherapy. Using complementary gene knockdown and gene overexpressing systems, we also showed that overexpression of NAC-1 was essential for paclitaxel resistance. Its role in Taxol resistance makes NAC-1 an attractive target for designing chemotherapeutic agents for patients resistant to conventional taxane-based regimens.

Disclosure of Potential Conflicts of Interest

No potential conflicts of interest were disclosed.

References

1. Wingo PA, Tong T, Bolden S, et al. Cancer statistics. CA Cancer J Clin 1995;45:8–30.
2. Agarwal R, Linch M, Kaye SB, et al. Novel therapeutic agents in ovarian cancer. Eur J Surg Oncol 2006; 32:875–86.
3. Stogios PJ, Downs, GS, Jauhal JJ, Nandra SK, Prive GG. Sequence and structural analysis of BTB domain proteins. Genome Biol 2005;6:R82.
4. Nakayama K, Nakayama N, Davidson B, et al. A BTB/POZ protein, NAC-1, is related to tumor recurrence and is essential for tumor growth and survival. Proc Natl Acad Sci U S A 2006;103:18739–44.
5. Wang J, Rao S, Chu J, et al. A protein interaction network for pluripotency of embryonic stem cells. Nature 2006;444:364–8.
6. Davidson B, Berner A, Trope CG, Wang TL, Shih Ie M. Expression and clinical role of the bric-a-brac tramtrack broad complex/poxvirus and zinc protein NAC-1 in ovarian carcinoma effusions. Hum Pathol 2007; 38:1030–6.
7. Yamamoto K, Kikuchi Y, Kudo K, Nagata I. Modulation of cisplatin sensitivity by taxol in cisplatin-sensitive and -resistant human ovarian carcinoma cell lines. J Cancer Res Clin Oncol 2000;126:168–72.
8. Nakayama K, Miyazaki K, Kanzaki A, Fukumoto M, Takebayashi Y. Expression and cisplatin sensitivity of copper-transporting P-type adenosine triphosphatase (ATP7B) in human solid carcinoma cell lines. Oncol Rep 2001;8:1285–7.
9. Albagli-Curiel O. Ambivalent role of BCL6 in cell survival and transformation. Oncogene 2003;22: 507–16.
10. Puccetti E, Zheng X, Brambilla D, et al. The integrity of the charged pocket in the BTB/POZ domain is essential for the phenotype induced by the leukemia-associated t(11;17) fusion protein PLZF/RARα. Cancer Res 2005;65:6080–8.
11. Liang XQ, Avraham HK, Jiang S, Avraham S. Genetic alterations of the NRP/B gene are associated with human brain tumors. Oncogene 2004;23:5890–900.
12. Reuter S, Bartelmann M, Vogt M, et al. APM-1, a novel human gene, identified by aberrant co-transcription with papillomavirus oncogenes in a cervical carcinoma cell line, encodes a BTB/POZ-zinc finger protein with growth inhibitory activity. EMBO J 1998;17:215–22.
13. van Roy FM, McCrea PD. A role for Kaiso-p120ctn complexes in cancer? Nat Rev Cancer 2005;5:956–64.
14. Valenta T, Lukas J, Doubravska L, Fafilek B, Korinek V. HIC1 attenuates Wnt signaling by recruitment of TCF-4 and β-catenin to the nuclear bodies. EMBO J 2006;25:2326–37.
15. Diaz-Montes TP, Bristow RE. Secondary cytoreduction for patients with recurrent ovarian cancer. Curr Oncol Rep 2005;7:451–8.
16. Harter P, du Bois A. The role of surgery in ovarian cancer with special emphasis on cytoreductive surgery for recurrence. Curr Opin Oncol 2005;17: 505–14.
17. Gadducci A, Iacconi P, Cosio S, Fanucchi A, Cristofani R, Riccardo Genazzani A. Complete salvage surgical cytoreduction improves further survival of patients with late recurrent ovarian cancer. Gynecol Oncol 2000;79: 344–9.
18. Gadducci A, Iacconi P, Fanucchi A, Cosio S, Teti G, Genazzani AR. Surgical cytoreduction during second-look laparotomy in patients with advanced ovarian cancer. Anticancer Res 2000;20:1959–64.
19. Zang RY, Li ZT, Tang J, et al. Secondary cytoreductive surgery for patients with relapsed epithelial ovarian carcinoma: who benefits? Cancer 2004;100: 1152–61.
20. Goto T, Takano M, Sakamoto M, et al. Gene expression profiles with cDNA microarray reveal RhoGDI as a predictive marker for paclitaxel resistance in ovarian cancers. Oncol Rep 2006;15:1265–71.
21. Britten RA, Perdue S, Eshpeter A, Merriam D. Raf-1 kinase activity predicts for paclitaxel resistance in TP53mut, but not TP53wt human ovarian cancer cells. Oncol Rep 2000;7:821–5.
22. Duan Z, Feller AJ, Toh HC, Makastorsis T, Seiden MV. TRAG-3, a novel gene, isolated from a taxol-resistant ovarian carcinoma cell line. Gene 1999;229:75–81.
23. Kavallaris M, Kuo DY, Burkhart CA, et al. Taxol-resistant epithelial ovarian tumors are associated with altered expression of specific β-tubulin isotypes. J Clin Invest 1997;100:1282–93.
24. Mozzetti S, Ferlini C, Concolino P, et al. Class III β-tubulin overexpression is a prominent mechanism of paclitaxel resistance in ovarian cancer patients. Clin Cancer Res 2005;11:298–305.
25. Nakayama K, Nakayama N, Wang TL, Shih Ie M. NAC-1 controls cell growth and survival by repressing transcription of Gadd45GIP1, a candidate tumor suppressor. Cancer Res 2007;67:8058–64.
26. Mabuchi S, Ohmichi M, Nishio Y, et al. Inhibition of NFκB increases the efficacy of cisplatin in *in vitro* and *in vivo* ovarian cancer models. J Biol Chem 2004;279: 23477–85.
27. Liu GH, Wang S, Wang B, Kong BH. Inhibition of nuclear factor-κB by an antioxidant enhances paclitaxel sensitivity in ovarian carcinoma cell line. Int J Gynecol Cancer 2006;16:1777–82.
28. Smith ML, Chen IT, Zhan Q, et al. Interaction of the p53-regulated protein Gadd45 with proliferating cell nuclear antigen. Science 1994;266: 1376–80.
29. Zhang W, Bae I, Krishnaraju K, et al. CR6: a third member in the MyD118 and Gadd45 gene family which functions in negative growth control. Oncogene 1999;18:4899–907.
30. Wang XW, Zhan Q, Coursen JD, et al. GADD45 induction of a G_2-M cell cycle checkpoint. Proc Natl Acad Sci U S A 1999;96:3706–11.
31. Park KC, Song KH, Chung HK, et al. CR6-interacting factor 1 interacts with orphan nuclear receptor Nur77 and inhibits its transactivation. Mol Endocrinol 2005; 19:12–24.
32. Tang G, Minemoto Y, Dibling B, et al. Inhibition of JNK activation through NF-κB target genes. Nature 2001;414:313–7.
33. Sudo T, Nitta M, Saya H, Ueno NT. Dependence of paclitaxel sensitivity on a functional spindle assembly checkpoint. Cancer Res 2004;64:2502–8.

殻付き微細気泡群を含む液体中における非線形波の伝播

Propagation of Nonlinear Wave in Liquid Containing Encapsulated Microbubbles

○金川 哲也, 北大工, 札幌市北区北 13 条西 8 丁目, E-mail: kanagawa@mech-me.eng.hokudai.ac.jp
矢野　猛, 阪大工, 吹田市山田丘 2-1, E-mail: yano@mech.eng.osaka-u.ac.jp
渡部 正夫, 北大工, 札幌市北区北 13 条西 8 丁目, E-mail: masao.watanabe@eng.hokudai.ac.jp
藤川 重雄, 北大工, 札幌市北区北 13 条西 8 丁目, E-mail: fujikawa@eng.hokudai.ac.jp

Tetsuya Kanagawa, Graduate School of Engineering, Hokkaido University, Sapporo 060-8628
Takeru Yano, Graduate School of Engineering, Osaka University, Suita 565-0871
Masao Watanabe, Graduate School of Engineering, Hokkaido University, Sapporo 060-8628
Shigeo Fujikawa, Graduate School of Engineering, Hokkaido University, Sapporo 060-8628

One-dimensional nonlinear waves in a liquid containing a number of spherical microbubbles are theoretically studied on the basis of a two-fluid model equations. The set of averaged equations consists of conservation laws of mass and momentum in gas and liquid phases, and the equation of motion of bubble wall. The compressibility of liquid phase is taken into account in the conservation laws and the equation of bubble wall motion, and this leads to the wave attenuation due to bubble oscillations. By using the method of multiple scales, Korteweg-de Vries-Burgers equation can be derived. The properties of the equation are discussed and compared to previous results based on different models on bubbly liquids.

1. はじめに

薬剤を内部に封入した殻付き微細気泡を患部近傍へと運搬させた後, 超音波照射によって殻の破壊を誘起させ, 薬剤を患部へ作用させるという, ドラッグデリバリーを利用した非侵襲がん治療技術 [1] が注目されている. 臨床現場においては, 殻の破壊を誘起させうるほどに強力な超音波を用いるといった観点から, そのふるまいを線形領域で把握することは不可能であり, 気泡振動と音波の非線形相互作用を詳細に把握することが強く望まれている. 本稿では, その最も基礎的な知見を得るために, 多数の微細気泡 (殻を有しない) を含む液体中を伝播する弱非線形波動に取り組む.

気泡流中を伝播する非線形波動に関する解析的研究は, 古くから多様な事例が報告されており, たとえば, 支配方程式系を分散性をともなう単一の非線形方程式である Korteweg-de Vries 方程式へと帰着させた研究 [2], さらに, これに粘性に起因する散逸性をも含めて K-dV-Burgers 方程式へと帰着させた例 [3] などが挙げられよう. しかしながら, これらの報告は, 液相を非圧縮性とみなすこと, また気相および液相の圧力を単一の変数として取り扱う (表面張力の無視) ことなど, 大胆ともいえる仮定の下での結果であり, 気泡流中を伝播する非線形波の精密な理解にはそぐうものではない. このように, 気泡流を記述するための従属変数の多さなどに起因する理論解析の困難さに阻まれ, その基礎的な知見ですら, いまだ不明瞭といえる状況にある.

本研究では, 体積平均化に基づく気泡流の支配方程式系を起点として, 初期に一様に気泡を含む圧縮性液体中を伝播する非線形波動を理論的に取り扱う. Egashira らによって提出された 3 圧力 2 流体モデルに基づく平均化方程式系 [4] は, 液相および気相の圧力, 密度, 流速にそれぞれ異なる従属変数を導入する点, なかでも圧力に対しては気相と液相の両者のみならず, 気泡の非線形振動によって誘起される気泡近傍液体の局所的高圧 (気液界面における液相圧力) をも, 単独の従属変数として組み込みうるという点で特徴的である. この方程式系を起点として, 静止液体中および気泡流中を伝播する線形分散波の解析がなされてきており [4][5], 本稿ではその非線形領域への拡張が実行される. 特異摂動法の利用, また従属変数群の 2 次までの展開を行った結果, 支配方程式系が, 圧縮性液体中での気泡振動に起因する分散ならびに散逸効果, また 2 次の非線形効果を記述しうる, 気泡径の摂動項を従属変数とする単一の Korteweg-de Vries-Burgers 方程式へと帰着されることが示される.

2. 問題の定式化

初期時刻において, 気泡径やボイド率を含むすべての物理量が一様状態にあるとする, 多数の球形微細気泡を含む静止液体を想定する. 液体中に設置された音源の振動によって平面音波が放射されている. 音波の波面に直交する方向に空間座標 x をとる (座標の原点 O を初期時刻における音源の位置に設置する) ことによって, 空間依存性が 1 次元とみなせる問題に定式化できる.

本解析において, とくに着目されるのは液相の圧縮性であり, その結果, 音響放射減衰 (気泡の非線形振動に起因) に基づく散逸効果の抽出などが帰着する. そのような観点から, 簡単のため, 液相と気相の粘性および熱伝導性, 気液界面を通じての熱および物質移動, 相変化, また体積力の存在は無視する. さらに, 気泡は任意の時刻および位置において球形を保ち, 合体, 分裂, 生成, 消滅は起こらないものとする.

2.1 基礎方程式系

波動伝播の解析に先立って, 気泡流の運動を支配する方程式系を導入してゆく. 本項で導入される諸変数および諸定数は, すべて無次元化されており, その定義は, のちの 2.2 項において詳述される.

気泡流の運動は, 質量および運動量の保存則を表す以下の体積平均化に基づく方程式系 [4] にしたがうものとする:

- 気相の質量保存則

$$\frac{\partial}{\partial t}(\alpha\rho_G) + \frac{\partial}{\partial x}(\alpha\rho_G u_G) = 0. \tag{1}$$

- 液相の質量保存則

$$\frac{\partial}{\partial t}[(1-\alpha)\rho_L] + \frac{\partial}{\partial x}[(1-\alpha)\rho_L u_L] = 0. \tag{2}$$

- 気相の運動量保存則

$$\frac{\partial}{\partial t}(\alpha\rho_G u_G) + \frac{\partial}{\partial x}\left(\alpha\rho_G {u_G}^2\right) + \kappa\alpha\frac{\partial p_G}{\partial x} = F. \quad (3)$$

- 液相の運動量保存則

$$\frac{\partial}{\partial t}\left[(1-\alpha)\rho_L u_L\right] + \frac{\partial}{\partial x}\left[(1-\alpha)\rho_L u_L^2\right] + \kappa(1-\alpha)\frac{\partial p_L}{\partial x} + \kappa P\frac{\partial \alpha}{\partial x} = -F. \quad (4)$$

ここに, t は時間, α は気相の体積率 (ボイド率), u は流速, ρ は流体の密度, p は圧力, P は気液界面における局所的な液相圧力であり, また下添え字 G と L は, それぞれ, 気相および液相に付随する体積平均化された変数を意味する.

運動量保存則 (3)(4) における, 相間の運動量輸送項 F としては, 液相の圧縮性を考慮できるように拡張された付加慣性力 [6]

$$F = -\beta_1\alpha\rho_L\left(\frac{D_G u_G}{Dt} - \frac{D_L u_L}{Dt}\right) - \beta_2\rho_L(u_G-u_L)\frac{D_G\alpha}{Dt} - \beta_3\alpha(u_G-u_L)\frac{D_G\rho_L}{Dt}, \quad (5)$$

を導入する. 係数 $\beta_1, \beta_2, \beta_3$ は, 通常すべて $1/2$ とおかれることが多いが, 本稿では具体的な値を与えずに式展開を進めてゆく.

また, 気相および液相に沿う Lagrange 微分 D_G/Dt および D_L/Dt は, それぞれ, 以下のように定義される演算子である:

$$\frac{D_G}{Dt} \equiv \frac{\partial}{\partial t} + u_G\frac{\partial}{\partial x}, \qquad \frac{D_L}{Dt} \equiv \frac{\partial}{\partial t} + u_L\frac{\partial}{\partial x}. \quad (6)$$

気泡の運動方程式として, 液相の圧縮性を考慮に含む Keller の方程式 [7] を導入する:

$$\left(1 - M\delta\frac{D_G R}{Dt}\right)R\frac{D_G^2 R}{Dt^2} + \frac{3}{2}\left(1 - \frac{M\delta}{3}\frac{D_G R}{Dt}\right)\left(\frac{D_G R}{Dt}\right)^2 = \frac{\kappa}{\delta^2}\left(1 + M\delta\frac{D_G R}{Dt}\right)P + \frac{M\kappa}{\delta}R\frac{D_G}{Dt}(p_L + P). \quad (7)$$

ここで, R は気泡径であり, また無次元パラメータである M, δ, κ の定義については 2.2 項において後述される. 式 (7) の導入に関して, 単一気泡を扱った原著 [7] においては, 1 変数の時間に関する導関数で表されていた項の演算子を D_G/Dt で置き換え, また, 気液界面における局所液相圧力 P の導入も行うなどの操作を経ている.

方程式系 (1)-(4) および (7) は, 以下に示す 4 つの補助的関係式を導入することによって閉じられる. まず, 熱力学的状態変数を関係づける式として, 気相にはポリトロープ変化の関係式

$$\frac{p_G}{p_{G0}} = \left(\frac{\rho_G}{\rho_{G0}}\right)^\gamma, \quad (8)$$

を (p_{G0} と ρ_{G0} は, それぞれ, 気相の初期圧力と初期密度, γ は気泡内気体のポリトロープ指数), 液相には Tait 型の状態方程式

$$\frac{p_L + B}{1 + B} = \rho_L^n, \quad (9)$$

をそれぞれ課す (B および n は物質定数). さらに, 気泡内気体の質量保存則

$$\rho_G R^3 = \rho_{G0}, \quad (10)$$

また, 気液界面でにおける圧力のつりあい (Laplace の式)

$$p_G - (p_L + P) = \frac{2\sigma}{R}, \quad (11)$$

を導入する (σ は表面張力).

9 本の式から構成される方程式系 (1)-(4) および (7)-(11) は, 9 つの従属変数 $\alpha, \rho_G, \rho_L, u_G, u_L, p_G, p_L, P, R$ に対して, 閉じた方程式系を形成している.

2.2 無次元化の定義

方程式系 (1)-(11) における諸変数は, すでに, 以下の定義にしたがって無次元化されている:

$$x = \frac{x^*}{L^*}, \quad t = \frac{U^* t^*}{L^*}, \quad u_G = \frac{u_G^*}{U^*}, \quad u_L = \frac{u_L^*}{U^*},$$
$$\rho_G = \frac{\rho_G^*}{\rho_{L0}^*}, \quad \rho_L = \frac{\rho_L^*}{\rho_{L0}^*}, \quad p_G = \frac{p_G^*}{p_{L0}^*},$$
$$p_L = \frac{p_L^*}{p_{L0}^*}, \quad P = \frac{P^*}{p_{L0}^*}, \quad R = \frac{R^*}{R_0^*}. \quad (12)$$

ここで, L^*, U^* はそれぞれ流れ場 (音場) の代表的な長さ, 速さスケールであり, これらに加え, 液相の有次元の初期密度と初期圧力 ρ_{L0}^*, p_{L0}^* および初期の気泡径 R_0^* を用いて無次元化を行っている. アスタリスク "$*$" を, すべての, 有次元変数および有次元定数に記してあることに注意されたい.

つづいて, 無次元諸定数の定義も示す:

$$\rho_{G0} = \frac{\rho_{G0}^*}{\rho_{L0}^*}, \quad p_{G0} = \frac{p_{G0}^*}{p_{L0}^*}, \quad B = \frac{B^*}{p_{L0}^*}, \quad \sigma = \frac{\sigma^*}{p_{L0}^* R_0^*}. \quad (13)$$

さらに, 無次元方程式系 (3)(4) および (7) に現れているパラメータ κ, M, δ は, 以下の定義によって導入されたものである:

$$\kappa = \frac{p_{L0}^*}{\rho_{L0}^* {U^*}^2}, \quad M = \frac{U^*}{c_{L0}^*}, \quad \delta = \frac{R_0^*}{L^*}. \quad (14)$$

ここに, c_{L0}^* は初期の液単相音速であり, また, δ とは流れ場の代表長さスケール (たとえば波長) に対する初期気泡径の比をあらわす.

ここで, 平均化方程式系を用いるにあたって重要となる空間スケールについて触れておく. 気泡流中の 4 つの長さスケール, すなわち, 気泡径, 気泡間距離, 平均化の長さスケール, 流れ場の代表長さスケール, これらについて, 以下の大小関係が成立していなければならない:

$$R_0^* \ll {n_0^*}^{-1/3} \ll {V^*}^{1/3} \ll L^*. \quad (15)$$

ここに, n_0^* は初期の気泡数密度 (したがって ${n_0^*}^{-1/3}$ とは初期の気泡間距離), V^* は平均化体積である. 不等式 (15) とは, 気泡半径が十分小さく, 平均化体積内に十分たくさんの気泡が含まれていて, かつ, 注目する波の運動スケールが平均化のスケールより大きいという要請である. したがって

$$\alpha_0 = \frac{4}{3}\pi {R_0^*}^3 n_0^* \ll 1, \quad (16)$$

なる関係が成立する. すなわち, 初期ボイド率 α_0 は, 1 に比べて十分に小さくなければならない.

3. 非線形波動を記述する単一方程式への帰着

3.1 摂動展開

方程式系 (1)-(4) および (7)-(11) における, 9 つの従属変数に対して, その大きさが $0 < \epsilon \ll 1$ とみなせるパラメータ ϵ を用いて, 以下のような展開をおこなう:

$$u_G = \epsilon u_{G1} + \epsilon^2 u_{G2} + \cdots, \quad (17)$$
$$u_L = \epsilon u_{L1} + \epsilon^2 u_{L2} + \cdots, \quad (18)$$
$$\rho_G = \rho_{G0}(1 + \epsilon\rho_{G1} + \epsilon^2\rho_{G2} + \cdots), \quad (19)$$

$$\rho_L = 1 + \epsilon\rho_{L1} + \epsilon^2\rho_{L2} + \cdots, \tag{20}$$
$$p_G = p_{G0}(1 + \epsilon p_{G1} + \epsilon^2 p_{G2} + \cdots), \tag{21}$$
$$p_L = 1 + \epsilon p_{L1} + \epsilon^2 p_{L2} + \cdots, \tag{22}$$
$$P = \epsilon P_1 + \epsilon^2 P_2 + \cdots, \tag{23}$$
$$R = 1 + \epsilon R_1 + \epsilon^2 R_2 + \cdots, \tag{24}$$
$$\alpha = \alpha_0(1 + \epsilon\alpha_1 + \epsilon^2\alpha_2 + \cdots). \tag{25}$$

ここで, たとえば, u_{G1}, u_{G2} などといった従属変数群の摂動項は, すべて $O(1)$ であると定める.

つづいて, 従属変数群の摂動項, たとえば, 気泡径 R の 1 次および 2 次の摂動項に関して, 以下のような独立変数依存性を仮定する (他の従属変数に関しても同様):

$$R_1 = R_1(x, t_0, t_1), \qquad R_2 = R_2(x, t_0). \tag{26}$$

ここに, 時間に関する独立変数について, t_0 と t_1 の両者が用意されているが, これらはそれぞれ

$$t_0 \equiv t, \qquad t_1 \equiv \epsilon t, \tag{27}$$

によって導入したものである. $\epsilon \ll 1$ であることから, $t_1 = \epsilon t$ とは, $t_0 = t$ にくらべて十分にゆるやかな (小さい) 変化を記述するのに適切な変数であることがわかる. 定義 (27) から, R_1 の t に関する偏導関数は以下のように展開される:

$$\frac{\partial R_1}{\partial t} = \frac{\partial R_1}{\partial t_0} + \epsilon\frac{\partial R_1}{\partial t_1}. \tag{28}$$

時間に関して, t_0 に支配される方程式 (あるいは項) は, 近傍場, すなわち解のふるまいがほぼ線形とみなせるような領域を記述し, いっぽう t_1 に支配される方程式は, 遠方場, すなわち蓄積した弱い非線形効果が無視できないような領域を記述する. 具体的には, 近傍場を記述する線形方程式が 3.3 項で, 遠方場を記述する非線形方程式が 3.4 項において, それぞれ導かれる.

3.2 諸変数と諸定数のオーダー設定

式 (13) や (14) などにおいてあらわれる, 無次元諸定数およびパラメータのオーダーを設定する:

$$\begin{aligned}
&\rho_{G0} = O(\epsilon^2), \quad p_{G0} = O(1), \quad \alpha_0 = O(1),\\
&B = O(1), \quad \sigma = O(1),\\
&M = O(\sqrt{\epsilon}), \quad \delta = O(\sqrt{\epsilon}), \quad \kappa = O(1).
\end{aligned} \tag{29}$$

ここで, 式 (29) における, $O(1)$ 以外の定数については

$$\delta \equiv \sqrt{\epsilon}\Delta_1, \quad M \equiv \sqrt{\epsilon}\Delta_2, \quad \rho_{G0} \equiv \epsilon^2\Delta_3, \tag{30}$$

とおいておく ($\Delta_1 = O(1), \Delta_2 = O(1), \Delta_3 = O(1)$ とする). なお, 本問題で着目する現象は, 最大で 2 次の摂動項が寄与するものであるため, ρ_{G0} からの寄与はないことは容易にわかる.

以上より, もともとの従属変数群 (17)-(25) のオーダーを, 以下のように見積もったこととなる:

$$\begin{aligned}
&u_G = O(\epsilon), \quad u_L = O(\epsilon), \quad \rho_G = O(\epsilon^2),\\
&\rho_L = O(1), \quad p_G = O(1), \quad p_L = O(1),\\
&P = O(\epsilon), \quad R = O(1), \quad \alpha = O(1).
\end{aligned} \tag{31}$$

まず, ϵ^0 を係数とする関係式として, 式 (9) および (11) から, ただちに以下の関係式群を得る:

$$c_{L0}^2 = \kappa n(1 + B), \qquad p_{G0} - 1 = 2\sigma. \tag{32}$$

ここに, $c_{L0} = c_{L0}^*/U^*$ は液単相の無次元初期音速である.

3.3 線形波動

保存則 (1)-(4) および Keller の方程式 (7) から, ϵ を係数とする項のみを取り出す. さらに, 変数の削減のために, 補助関係式 (8)-(11) を適切に用いれば, $\alpha_1, u_{G1}, u_{L1}, p_{L1}, R_1$ のみを未知変数とする方程式系を得る:

$$\frac{\partial\alpha_1}{\partial t_0} - 3\frac{\partial R_1}{\partial t_0} + \frac{\partial u_{G1}}{\partial x} = 0, \tag{33}$$
$$\frac{\kappa}{c_{L0}^2}\frac{\partial p_{L1}}{\partial t_0} - \frac{\alpha_0}{1-\alpha_0}\frac{\partial\alpha_1}{\partial t_0} + \frac{\partial u_{L1}}{\partial x} = 0, \tag{34}$$
$$\beta_1\frac{\partial u_{G1}}{\partial t_0} - \beta_1\frac{\partial u_{L1}}{\partial t_0} - 3\gamma\kappa p_{G0}\frac{\partial R_1}{\partial x} = 0, \tag{35}$$
$$\frac{1-\alpha_0+\beta_1\alpha_0}{1-\alpha_0}\frac{\partial u_{L1}}{\partial t_0} - \frac{\beta_1\alpha_0}{1-\alpha_0}\frac{\partial u_{G1}}{\partial t_0} + \kappa\frac{\partial p_{L1}}{\partial x} = 0, \tag{36}$$
$$p_{L1} + \omega_B^2 R_1 = 0. \tag{37}$$

ここに, $\omega_B^2 = 3\gamma p_{G0} - 2\sigma = O(1)$ は, 単一気泡の無次元固有角振動数である.

方程式系 (33)-(37) は, いくらかの計算を経て, 単一変数 R_1 に対する線形波動方程式

$$\frac{\partial^2 R_1}{\partial t_0^2} - v_p^2\frac{\partial^2 R_1}{\partial x^2} = 0, \tag{38}$$

へと帰着させることができる. これが近傍場を記述する方程式である. ここに, v_p は位相速度であり, $\alpha_0, \kappa, \omega_B$ などといった $O(1)$ の諸定数を用いて表現される (本稿ではその依存形は省略する).

3.4 分散性と散逸性をあわせもつ非線形波動

式 (38) における位相速度を用いて, 新たな独立変数 φ を

$$\varphi \equiv x - v_p t_0, \tag{39}$$

によって導入すれば, 時間 t_0 および空間座標 x に対する偏微分演算子が, 以下のように変数変換される:

$$\frac{\partial}{\partial t_0} = -v_p\frac{\partial}{\partial\varphi}, \qquad \frac{\partial}{\partial x} = \frac{\partial}{\partial\varphi}. \tag{40}$$

したがって, このとき仮に, 従属変数が R_1 以外であっても, 線形波動方程式 (38) の左辺は恒等的にゼロとなる. 変数 φ の導入とは, x 軸正方向へと一定速度 v_p で進行する波の存在の仮定に対応する. また, 式 (26) を, 以下のように表現し直しておく:

$$R_1 = R_1(\varphi, t_1), \qquad R_2 = R_2(\varphi). \tag{41}$$

遠方場を記述する方程式を抽出するために, 方程式系 (1)-(4) および (7) から, ϵ^2 を係数とする項を取り出し, 3.3 項と同じく変数の削減も行うことによって, 以下の方程式系を得る:

$$\frac{\partial}{\partial\varphi}[u_{G2} - v_p(\alpha_2 - 3R_2)] = f_1, \tag{42}$$
$$\frac{\partial}{\partial\varphi}\left[u_{L2} - v_p\left(\frac{\kappa}{c_{L0}^2}p_{L2} - \frac{\alpha_0}{1-\alpha_0}\alpha_2\right)\right] = f_2, \tag{43}$$
$$\frac{\partial}{\partial\varphi}[v_p\beta_1(u_{L2} - u_{G2}) - 3\gamma\kappa p_{G0}R_2] = f_3, \tag{44}$$
$$\frac{\partial}{\partial\varphi}\left[\kappa p_{L2} - \frac{v_p\{(1-\alpha_0+\beta_1\alpha_0)u_{L2} - \beta_1\alpha_0 u_{G2}\}}{1-\alpha_0}\right] = f_4, \tag{45}$$
$$p_{L2} + \omega_B^2 R_2 = f_5. \tag{46}$$

方程式系 (42)-(46) は, 3.3 項の手順に倣えば, 気泡径の 1 次摂動項 R_1 を従属変数とする単一方程式にまとめあげることが可能である. その際, 以下の事項を用いて計算をすすめる:

1. 上記単一方程式の左辺は, R_2 が従属変数であることを除いて, 線形波動方程式 (38) と同形であるが, すでに, 変数 φ を導入したことによって自動的にゼロとなる.
2. 近傍場を記述する方程式系 (33)-(36) を, φ に対する偏導関数のみから構成される偏微分方程式としてまとめ直した後に, φ に関する不定積分を行い, 従属変数間を関係付ける代数関係式群を得る.
3. 方程式系 (42)-(46) における, 独立変数として φ と t_1 にしたがう非同次項 f_i ($i = 1, 2, 3, 4, 5$) は, $\alpha_1, u_{G1}, u_{L1}, p_{L1}, R_1$ の, φ に関する 2 次の偏導関数項, および, t_1 に関する 1 次の偏導関数項の線形結合から形成されるが, この両者ともに, 事項 2. の利用によって, 単一変数 R_1 の偏導関数項のみで表現し直すことが可能である.

上記の操作を実行することによって, 遠方場を記述する, 単一の 3 階非線形偏微分方程式を導出することができる:

$$\frac{\partial R_1}{\partial t_1} + C_1 R_1 \frac{\partial R_1}{\partial \varphi} + C_2 \frac{\partial^2 R_1}{\partial \varphi^2} + C_3 \frac{\partial^3 R_1}{\partial \varphi^3} = 0. \qquad (47)$$

ここに, C_1, C_2, C_3 は諸定数から形成される係数であるが, その陽的な形は本稿では差し控える.

式 (47) は, 気泡流中において, 分散性と散逸性ならびに 2 次の非線形性をあわせもつ波動現象を記述する Korteweg-de Vries-Burgers 方程式である. 線形波動方程式 (38) および K-dV-Burgers 方程式 (47) は, 近傍場においては無視できた分散, 散逸, 非線形の効果が, 遠方場において, 同時に発現しうることを示している. 諸定数のオーダーの適切な選定 (29) のもとで, 3 圧力 2 流体モデルに基づく質量および運動量の保存則 (1)-(4), および Keller の方程式 (7) という, 5 本もの偏微分方程式系の 5 つの従属変数群の 2 次摂動項を考慮することによって, 式 (47) の導出に至ることができた.

その導出過程をふりかえればわかるように, 分散項は Keller の方程式の 2 階導関数項 (左辺第 1 項) に起因し, 散逸項は 1 階導関数 (音響放射減衰) 項 (右辺第 2 項) に起因する. また, 非線形項は, 4 つの保存則および Keller の方程式のすべてに起因している. なかでも, 散逸項が, 媒質の粘性や熱伝導性に起因するのではなく, 液相圧縮性の効果による, 気泡の減衰振動 (音響放射減衰) に起因することは, 特筆すべき差異である. 液相を非圧縮性とみなして, K-dV-Burgers 方程式の導出を試みた既知研究 [3] においては, その散逸項は, 粘性あるいは熱伝導性にしか由来しえないからである.

従来の解析との差異のより精密な比較, また諸係数 C_1, C_2, C_3 の定義など, 詳細は講演時に述べる.

4. 今後の展望

第 1 の展望として, K-dV-Burgers 方程式 (47) を数値的に解くことによって, そのふるまいの把握, とくに非線形効果, 散逸効果, 分散効果の定量的把握をすることが挙げられる. また, 音響放射減衰のみならず, 流体の粘性および熱伝導性の考慮による散逸効果をも含む K-dV-Burgers 方程式の導出も展望である.

さらに, はじめに述べたように, 医療応用を見据えるという目的からは, 殻付き気泡の振動特性を踏まえる必要がある. すでに, Hoff らが, 非圧縮性液体中における単一の粘弾性殻付き球形気泡の振動を記述する方程式 [1] を導いている:

$$\rho_L^* \left[R^* \frac{\mathrm{d}^2 R^*}{\mathrm{d}t^{*2}} + \frac{3}{2} \left(\frac{\mathrm{d}R^*}{\mathrm{d}t^*} \right)^2 \right] = P^* - 12 \frac{d_0^* R_0^*}{R^{*3}} \left[G_s^* \left(1 - \frac{R_0^*}{R^*} \right) + \frac{\mu_s^*}{R^*} \frac{\mathrm{d}R^*}{\mathrm{d}t^*} \right]. \qquad (48)$$

ここに, d_0^* は初期静止平衡状態における殻の厚さ, また G_s^* と μ_s^* は, それぞれ, 殻の振動に起因する剛性率 (横弾性係数) および粘性率である (他記号の定義は本稿中の記述と同一, また諸変数と係数はすべて有次元).

式 (48) は, 液相の粘性および表面張力を無視した Rayleigh-Plesset の式 (左辺, および右辺第 1 項が相当する) と, 殻の弾性に起因する項 (右辺第 2 項), また殻の粘性に起因する項 (右辺第 3 項), これらの線形結合により形成されている. 殻の弾性および粘性の効果を考慮した上での気泡振動の, 波のふるまいへ与える影響を, 定性的および定量的に知ることが強く望まれる.

本稿では, 殻の存在自体を考慮しなかったが, 今後, 圧縮性を考慮した液体中における殻付き気泡の振動を記述する方程式を, Hoff ら [1] や Keller ら [7] に倣って導出することを試み, 支配方程式系に組み込み直すことによって, 本理論の医学への応用をも目指す.

謝辞

本研究は, 平成 20 度厚生労働省科学研究費補助金 (医療機器開発推進研究事業: ナノメディシン研究 (H19-nano-010) によりなされたものである. ここに記して謝意を表す.

参考文献

(1) Hoff, L., Sontum, P. C. and Hovem, J. M., "Oscillations of polymeric microbubbles: Effect of the Encapsulating Shell," *J. Acoust. Soc. Am.*, **107** (2000), pp. 2272–2280.

(2) van Wijingaarden, L., "On the equation of motion for mixtures of liquid and gas bubbles," *J. Fluid. Mech.*, **33** (1968), pp. 465–474.

(3) van Wijingaarden, L., "One-dimensional flow of liquids containing small gas bubbles," *Annu. Rev. Fluid Mech.*, **4** (1972), pp. 369–396.

(4) Egashira, R., Yano, T. and Fujikawa, S., "Linear wave propagation of fast and slow modes in mixtures of liquid and gas bubbles," *Fluid Dyn. Res.*, **34** (2004), pp. 317–334.

(5) Yano, T., Egashira, R. and Fujikawa, S., "Linear analysis of dispersive waves in bubbly flows based on averaged equations," *J. Phys. Soc. Jpn.*, **75** (2006), pp. 104401-01-08.

(6) Eames, I. and Hunt, J. C. R., "Forces on bodies moving unsteadily in rapidly compressed flows," *J. Fluid Mech.*, **505** (2004), pp. 349–364.

(7) Keller, J. B. and Miskis, M., "Bubble oscillations of large amplitude," *J. Acoust. Soc. Am.*, **68** (1980), pp. 628–633.

Proceedings of CAV2009
Seventh International Symposium on Cavitation
August 17-22, 2009, Ann Arbor, Michigan, USA

WEAKLY NONLINEAR ANALYSIS OF DISPERSIVE WAVES IN MIXTURES OF LIQUID AND GAS BUBBLES BASED ON A TWO-FLUID MODEL

Tetsuya KANAGAWA
Division of Mechanical & Space Engineering
Hokkaido University, Sapporo, Japan
kanagawa@mech-me.eng.hokudai.ac.jp

Takeru YANO
Division of Mechanical Engineering
Osaka University, Suita, Japan
yano@mech.eng.osaka-u.ac.jp

Masao WATANABE
Division of Mechanical & Space Engineering
Hokkaido University, Sapporo, Japan
masao.watanabe@eng.hokudai.ac.jp

Shigeo FUJIKAWA
Division of Mechanical & Space Engineering
Hokkaido University, Sapporo, Japan
fujikawa@eng.hokudai.ac.jp

ABSTRACT

The characteristics of sound waves in bubbly liquids are considerably different from those in single phase fluids [1,2]. Especially, the dispersion in the sense that waves of different wavelengths propagate with different phase velocities is an important property, which is caused by bubble oscillations.

In the present paper, the one-dimensional nonlinear dispersive waves in the liquid containing a number of small spherical gas bubbles (see Fig. 1) are theoretically studied on the basis of a set of two-fluid averaged equations derived by the present authors [3,4]. The set of equations is composed of the conservation laws of mass and momentum for gas and liquid phases [3], the Keller equation of the oscillations of spherical gas bubble [5], the equations of state for gas and liquid phases, the law of mass conservation of the gas inside each bubble, and the pressure balance at the gas-liquid interface. At an initial state, the mixtures are assumed to be uniform and at rest. The compressibility of liquid phase is taken into account. For the simplicity, we neglect the viscosity, thermal conductivity, phase change across the interface, and Reynolds stress.

Egashira *et al.* [3] analyzed linear pressure waves in the bubbly liquid on the basis of the two-fluid model, and showed the existence of the two modes, i.e., slow mode and fast mode, by

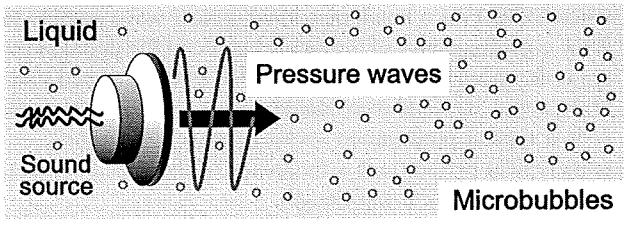

Figure 1. Schematic of the problem. Pressure waves in the liquid containing a number of small spherical gas bubbles generated by oscillations of the sound source. The mixtures are uniform and at rest at an initial state.

considering the compressibility of liquid. Figure 2 shows the linear dispersion relation of slow mode [3]. Band A and Band B in Fig. 2 are correspondent to the moderately low and high frequency bands, respectively. Here, Band A is regarded as the weakly dispersive band. We firstly analyze the weakly nonlinear propagation of pressure waves in Band A by an appropriate scaling of parameters.

Now, let us define the scaling of three parameters, i.e., the characteristics velocity U, the characteristics length L, and the

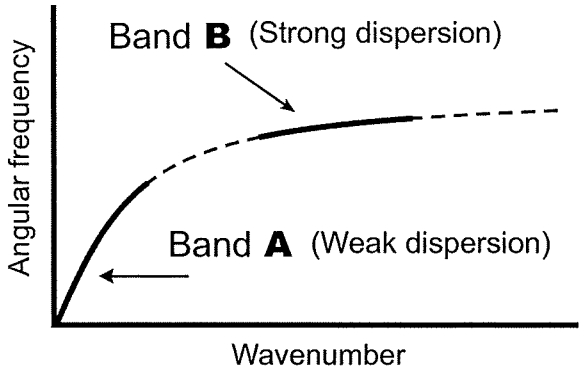

Figure 2. The dispersion relation of the slow mode in a bubbly quiescent liquid [3]. Band A and Band B indicate the weakly and strongly dispersive bands, respectively.

characteristics time T, as follows:

$$T\omega_B\sqrt{\varepsilon} \equiv O(1) \equiv \Omega, \tag{1}$$

$$\frac{U}{c_{L0}\sqrt{\varepsilon}} \equiv O(1) \equiv V, \tag{2}$$

$$\frac{R_0}{L\sqrt{\varepsilon}} \equiv O(1) \equiv \Delta, \tag{3}$$

where $\varepsilon(\ll 1)$ is a nondimensional typical wave amplitude, ω_B is the eigenfrequency of the single bubble of the initial radius R_0, c_{L0} is the speed of sound in the liquid in an unperturbed state, and Ω, V, and Δ are nondimensional constants of $O(1)$. The velocity U is a typical propagation speed of waves, the time $T = 1/\omega$ is its typical period (ω is a frequency of the sound source), and $L = UT$ is its typical wavelength.

All dependent variables are nondimensionalized and then expanded in a power series of ε. Here, we shall remark that only the perturbation expansion of the density of liquid phase begins with $O(\varepsilon^2)$. By substituting the expansions into the system of governing equations and using the scalings (1)-(3), we can derive the equation of the near field characterized by L and T. As a result, the near field is described by the linear wave equation. Therefore, the near field can be regarded as a nondispersive and nondissipative region in the present analysis based on the scalings (1)-(3).

Let us proceed to the derivation of equation in a far field, where the weak dispersion effect and weak dissipation effect appear and compete with the weak nonlinear effect. We shall introduce the two time scales $t_0 = t$ and $t_1 = \varepsilon t$ (t is the nondimensional time). The far field equation, the Korteweg–de Vries–Burgers (KdV-Burgers) equation can be derived by the use of multiple scales, as follows:

$$\frac{\partial f}{\partial t_1} + C_1 f\frac{\partial f}{\partial \varphi} + C_2\frac{\partial^2 f}{\partial \varphi^2} + C_3\frac{\partial^3 f}{\partial \varphi^3} = 0, \tag{4}$$

where $\varphi = x - vt_0$ is the nondimensional phase angle of the right-running wave (x is the nondimensional space coordinate normal to the wavefront, $v = 1 - \varepsilon\Omega^2V^2\Delta^2(1-\alpha_0)/(6\alpha_0)$ is the phase velocity of waves in the far field, and α_0 is the void fraction in the unperturbed state), and $f(t_1, \varphi)$ is the leading order approximation of the nondimensional bubble radius. Here, the coefficients of dissipative and dispersive terms in Eq. (4), C_2 and C_3 are given by

$$C_2 = -\frac{\Omega^2V\Delta^3}{6\alpha_0}, \quad C_3 = \frac{\Delta^2}{6\alpha_0}. \tag{5}$$

The explicit representation of the coefficient C_1 will be shown in the final technical paper because of the complexity of expression.

The KdV-Burgers equation (4) describes the weakly nonlinear propagation of waves with dissipative and dispersive effects. The third term in Eq. (4) is derived from the effect of the attenuation of bubble oscillations due to acoustic radiation, i.e., the consideration of the compressibility of liquid phase.

Furthermore, the propagation of linear pressure waves in the moderately high frequency band (see Band B in Fig. 2), which have strongly dispersive effects, is analyzed by the present authors [6]. We extend the problem to the weakly nonlinear problem. The result will be shown in the final technical paper.

ACKNOWLEDGEMENTS

This work was carried out by the aid of Research on Advanced Medical Technology, Ministry of Health, Labor and Welfare (H19-nano-010). The authors would like to express their deepest gratitude towards this grant.

REFERENCES

[1] van Wijingaarden, L., 1968, *J. Fluid Mech.*, **33**, 465-474.
[2] van Wijingaarden, L., 1972, *Annu. Rev. Fluid Mech.*, **4**, 369-396.
[3] Egashira, R., Yano, T. and Fujikawa, S., 2004, *Fluid Dyn. Res.*, **34**, 317-334.
[4] Yano, T., Egashira, R. and Fujikawa, S., 2006, *J. Phys. Soc. Jpn.*, **75**, 104401-01-08.
[5] Keller, J. B. and Kolodner, I. I., 1956, *J. Appl. Phys.*, **27**, 1152-1161.
[6] Haga, T., Yano, T. and Fujikawa, S., 2008, *Proc. 7th JSME-KSME Thermal and Fluids Engineering Conference*, Japan.

キャビテーションに関するシンポジウム (第 14 回)
2009.3.19–20・仙台市

2 流体モデルに基づく気泡含有液体中を伝播する分散性波動に対する弱非線形解析

Weakly Nonlinear Analysis of Dispersive Waves in Bubbly Liquid Based on Two-Fluid Model

○ 金川 哲也 (北大)　矢野　猛 (阪大)　渡部 正夫 (北大)　藤川 重雄 (北大)

Tetsuya Kanagawa, Graduate School of Engineering, Hokkaido University, Sapporo, 060-8628
Takeru Yano, Graduate School of Engineering, Osaka University, Suita, 565-0871
Masao Watanabe, Graduate School of Engineering, Hokkaido University, Sapporo, 060-8628
Shigeo Fujikawa, Graduate School of Engineering, Hokkaido University, Sapporo, 060-8628

One-dimensional nonlinear dispersive waves in a bubbly liquid is studied theoretically based on a two-fluid model composed of the conservation laws of mass and momentum for gas and liquid phases, and the Keller equation for the dynamics of the spherical bubble. The compressibility of the liquid phase is taken into account, and this leads to the wave attenuation due to bubble oscillations. We focus on the moderately high frequency band regarded as the strongly dispersive band. By using the method of multiple scales, we can derive the nonlinear Schrödinger equation with an attenuation term due to acoustic radiation from bubbles. This equation describes a far field of nearly monochromatic wave train in bubbly liquids, which evolves into a slowly modulated wave packet as a result of long range propagation of weakly nonlinear waves with strong dispersion effect.

Keywords: Weakly nonlinear wave, Bubbly liquid, Strong dispersion, Acoustic radiation, Nonlinear Schrödinger equation

1 はじめに

Egashira らによって, キャビテーションによって生じる気泡近傍の局所的高圧や, 気泡を含む圧縮性液体中に放射される強い圧力波を記述できる, 2 流体モデルに基づく気泡流の方程式系が導出された [1]. われわれは, この方程式を起点とした, 線形波動伝播の解析を行ってきた [1, 2].

また, 非線形効果を取り入れた解析として, 球形微細気泡を多数含む圧縮性液体中における, 波長の長い圧力変動が, 気泡の固有振動数に比べて小さな周波数のもとで伝播するとき, 十分な距離を伝播した後におけるふるまいが K-dV-Burgers 方程式で記述されることを示した [3]. さらに, 気泡の固有振動数と圧力変動の周波数が同程度, および, 波長が短い圧力波に対する線形伝播過程を調べた [4]. これらの両解析において, 分散性の効果が, 前者の問題設定 [3] では波長に比べ十分な距離を伝播するまではあらわれないのに対し, 後者の設定 [4] においては数波長程度の距離を伝播する間にあらわれる. 比較するならば, 後者は, 前者より強い分散性を示す周波数帯に注目しているといえる.

一般に, ある種の強分散性媒質中において, 特定の波数および周波数のまわりに狭い広がりを持つ準単色波列を考える. このとき, 弱い非線形効果も考慮すると, 搬送波はゆるやかな変化を受け, 搬送波の包絡線の振幅の時間発展は, 非線形 Schrödinger 方程式によって記述される [5]. 非線形 Schrödinger 方程式の 1 つの定常進行波解として, 図 1 に, 包絡ソリトン (または, ブライトソリトン) の波形を示す.

本報告では, 先の報告 [4] を, 非線形問題へ拡張し, 多数の微細気泡を含む圧縮性液体中における高周波数および短波長の, 準単色波列の非線形効果による変調を取り扱う. その過程は, 非線形 Schrödinger 方程式に, 液相の圧縮性に由来する音響放射減衰に伴う項を付加した式で記述されることが示される.

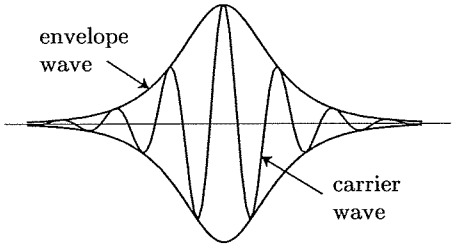

Fig. 1: Waveform of the envelope soliton as a solution of the nonlinear Schrödinger equation.

2 問題設定および基礎方程式

多数の微細な球形気泡を含む液体中に音源が設置されており, その位置を原点 O とする 1 次元空間座標 x^* を設定する. 音源から, 角振動数 ω^* のもとで, x^* 軸の正方向へ, 平面波が放射されている状況を考える. なお, $*$ を, すべての有次元変数および有次元定数に付けて, 無次元量と区別する.

2.1 基礎方程式系　気泡流の運動は, Egashira らによって提案された, 2 流体モデルに基づく気相と液相それぞれに対する質量および運動量の保存則 [1] で記述される :

$$\frac{\partial}{\partial t^*}(\alpha\rho_G^*) + \frac{\partial}{\partial x^*}(\alpha\rho_G^* u_G^*) = 0, \tag{1}$$

$$\frac{\partial}{\partial t^*}[(1-\alpha)\rho_L^*] + \frac{\partial}{\partial x^*}[(1-\alpha)\rho_L^* u_L^*] = 0, \tag{2}$$

$$\frac{\partial}{\partial t^*}(\alpha\rho_G^* u_G^*) + \frac{\partial}{\partial x^*}\left(\alpha\rho_G^* {u_G^*}^2\right) + \alpha\frac{\partial p_G^*}{\partial x^*} = F^*, \tag{3}$$

$$\frac{\partial}{\partial t^*}[(1-\alpha)\rho_L^* u_L^*] + \frac{\partial}{\partial x^*}\left[(1-\alpha)\rho_L^* {u_L^*}^2\right] + (1-\alpha)\frac{\partial p_L^*}{\partial x^*} + P^*\frac{\partial \alpha}{\partial x^*} = -F^*, \tag{4}$$

ここに, t^* は時間, x^* は 1 次元空間座標 (波面に垂直), α は気相の体積率 (ボイド率), u^* は流速, ρ^* は流体の密度, p^* は圧力, P^* は気液界面における局所的な液相圧力, F^* は単位時間・単位体積あたりの気液の相間の運動量輸送を表し, また下添え字 G と L は, それぞれ, 気相に属する変数と液相に属する変数を意味する.

運動量保存則 (3)(4) の右辺における相間の運動量輸送項 F^* には, 液相の圧縮性を考慮できるように拡張された付加慣性力 [6] を考慮したモデル [2]

$$F^* = -\beta_1 \alpha \rho_L^* \left(\frac{\mathrm{D}_G u_G^*}{\mathrm{D}t^*} - \frac{\mathrm{D}_L u_L^*}{\mathrm{D}t^*} \right) - \beta_2 \rho_L^* (u_G^* - u_L^*) \frac{\mathrm{D}_G \alpha}{\mathrm{D}t^*} - \beta_3 \alpha (u_G^* - u_L^*) \frac{\mathrm{D}_G \rho_L^*}{\mathrm{D}t^*}, \quad (5)$$

を採用する. ここに, 係数 β_i $(i = 1, 2, 3)$ はふつう 3 つとも 1/2 とすればよく, また, $\mathrm{D}_G/\mathrm{D}t^*$ と $\mathrm{D}_L/\mathrm{D}t^*$ は, それぞれ, 以下のように定義される :

$$\frac{\mathrm{D}_G}{\mathrm{D}t^*} \equiv \frac{\partial}{\partial t^*} + u_G^* \frac{\partial}{\partial x^*}, \quad \frac{\mathrm{D}_L}{\mathrm{D}t^*} \equiv \frac{\partial}{\partial t^*} + u_L^* \frac{\partial}{\partial x^*}. \quad (6)$$

気泡壁の運動方程式として, 圧縮性液体中における気泡の膨張・収縮運動を記述できる, Keller の方程式 [7]

$$\left(1 - \frac{1}{c_{L0}^*} \frac{\mathrm{D}_G R^*}{\mathrm{D}t^*}\right) R^* \frac{\mathrm{D}_G^2 R^*}{\mathrm{D}t^{*2}} + \frac{3}{2} \left(1 - \frac{1}{3c_{L0}^*} \frac{\mathrm{D}_G R^*}{\mathrm{D}t^*}\right) \left(\frac{\mathrm{D}_G R^*}{\mathrm{D}t^*}\right)^2 = \left(1 + \frac{1}{c_{L0}^*} \frac{\mathrm{D}_G R^*}{\mathrm{D}t^*}\right) \frac{P^*}{\rho_{L0}^*} + \frac{R^*}{\rho_{L0}^* c_{L0}^*} \frac{\mathrm{D}_G}{\mathrm{D}t^*} (p_L^* + P^*), \quad (7)$$

を用いる. ここに, R^* は気泡径であり, c_{L0}^* および ρ_{L0}^* は, それぞれ, 初期静止状態における液相の音速および密度である. 式 (7) の右辺第 2 項が, 音響放射減衰の効果を表す.

その他の従属変数として, p_G^*, p_L^*, P^*, ρ_G^* は, 以下に示す, 気相に対するポリトロープ変化の関係式, 液相に対する状態方程式 (Tait の式を変形したもの), 気液界面における圧力のつりあい式, 気泡内気体の質量保存則から計算される :

$$p_G^* = \left(\frac{\rho_G^*}{\rho_{G0}^*}\right)^\gamma p_{G0}^*, \quad (8)$$

$$p_L^* = p_{L0}^* + \frac{\rho_{L0}^* c_{L0}^{*2}}{n} \left[\left(\frac{\rho_L^*}{\rho_{L0}^*}\right)^n - 1 \right], \quad (9)$$

$$P^* = p_G^* - p_L^* - \frac{2\sigma^*}{R^*}, \quad (10)$$

$$\rho_G^* = \left(\frac{R_0^*}{R^*}\right)^3 \rho_{G0}^*, \quad (11)$$

ここに, ρ_{G0}^*, p_{G0}^*, p_{L0}^* は, それぞれ, 初期状態における気相密度, 気相圧力, 液相圧力, σ^* は表面張力, γ はポリトロープ指数, n は物質定数である.

初期に, 媒質は静止状態にあり, また気泡径を含むすべての物理量が一様であるとする. さらに, 媒質の粘性, 熱伝導性, また気液界面を通しての相変化および物質輸送を無視する.

2.2 高周波数, 短波長の弱非線形波動 以下に示す 5 つの従属変数について, 波の代表的な無次元振幅 ϵ $(\ll 1)$ を用いて, 摂動展開する :

$$\alpha/\alpha_0 = 1 + \epsilon\alpha_1 + \epsilon^2 \alpha_0 + \cdots, \quad (12)$$

$$u_G^*/U^* = \epsilon u_{G1} + \epsilon^2 u_{G2} + \cdots, \quad (13)$$

$$u_L^*/U^* = \epsilon u_{L1} + \epsilon^2 u_{L2} + \cdots, \quad (14)$$

$$R^*/R_0^* = 1 + \epsilon R_1 + \epsilon^2 R_2 + \cdots, \quad (15)$$

$$\rho_L^*/\rho_{L0}^* = 1 + \epsilon^3 \rho_{L1} + \epsilon^4 \rho_{L2} + \cdots, \quad (16)$$

ここに, α_0 と R_0^* は, それぞれ, 初期状態におけるボイド率と気泡径, U^* は波の代表的な速さである. また, 無次元液相密度 ρ_L^*/ρ_{L0}^* の展開を, $O(\epsilon^3)$ から始めることを注意しておく.

場を特徴づける, 代表的なスケールとしての速度 U^*, 長さ L^*, 時間 T^* に対して, それぞれ

$$\frac{\omega^*}{\omega_B^*} \equiv O(1) \equiv \Omega, \quad (17)$$

$$\frac{R_0^*}{L^*} \equiv O(1) \equiv \Delta, \quad (18)$$

$$\frac{U^*}{\epsilon\, c_{L0}^*} \equiv O(1) \equiv V, \quad (19)$$

と定める. ここに, 波の代表的なスケールとして, T^* は周期, L^* は波長, $U^* = L^*/T^*$ は伝播速度を表す. また, Ω, Δ, V はすべて $O(1)$ の定数であり, ω_B^* は半径 R_0^* の単一気泡の固有角振動数 (減衰なし) である :

$$\omega_B^* \equiv \sqrt{\frac{3\gamma p_{G0}^* - 2\sigma^*/R_0^*}{\rho_{L0}^* R_0^{*2}}}. \quad (20)$$

オーダー評価 (17)-(19) は, それぞれ, 波の周波数が気泡の固有振動数と同程度であること, 波の波長が気泡径と同程度であること, 波の伝播速度の液単相音速に対する比率が $O(\sqrt{\epsilon})$ 程度の大きさであることを意味する. ここで, 平均化方程式 (1)-(4) は, ふつうは, (18) で定められるような短波は記述できないが, 平面波問題においては, 波面に平行な方向に, 多数の気泡が含まれるような十分に大きい平均化体積を設置可能であることから, 本問題に適用可能といえる [4].

液相圧力 p_L^* は, 式 (16), (9) および (19) を用いて

$$p_L^* = p_{L0}^* + \epsilon \rho_{L0}^* U^{*2} p_{L1} + \epsilon^2 \rho_{L0}^* U^{*2} p_{L2} + \cdots, \quad (21)$$

と展開される. ここに, 無次元液相圧力 p_{Li} $(i = 1, 2, 3)$ は, 定数 V を用いて, 無次元液相密度と結びつけて

$$p_{L1} = \frac{\rho_{L1}}{V^2}, \quad p_{L2} = \frac{\rho_{L2}}{V^2}, \quad p_{L3} = \frac{\rho_{L3}}{V^2}, \quad (22)$$

と導入している. なお, 本稿では p_{L3} までしか現れないが, p_{L4} は ρ_{Li} $(i = 1, 2, 3, 4)$ を用いて表されることを注意しておく (さらに高次のものも同様).

波の代表的な周期 T^* を, 気泡の固有角振動数 ω_B^* の逆数を用いて定める :

$$T^* \equiv \frac{1}{\omega_B^*}. \quad (23)$$

また, 初期静止状態における気相圧力 p_{G0}^* を

$$\hat{p}_{G0} \equiv \frac{p_{G0}^*}{\rho_{L0}^* U^{*2}} \equiv O(1), \quad (24)$$

のように無次元化およびオーダー評価し ($\hat{p}_{G0}$ は無次元の初期気相圧力), さらに, 初期液相密度に対する初期気相密度の比が, $O(\epsilon^3)$ 程度の小ささであると仮定する :

$$\frac{\rho_{G0}^*}{\rho_{L0}^*} \equiv O(\epsilon^3). \quad (25)$$

3 特異摂動法による解析

3.1 多重尺度法 [8] 時間 t^*, および, 空間座標 x^* を

$$t^* = T^* t, \quad x^* = L^* x, \tag{26}$$

と無次元化し, 無次元振幅 ϵ を用いて, 無次元時間 t と無次元空間座標 x に対する, slow variables を定義する：

$$\begin{aligned} &t_0 = t, \quad t_1 = \epsilon t, \quad t_2 = \epsilon^2 t, ... \\ &x_0 = x, \quad x_1 = \epsilon x, \quad x_2 = \epsilon^2 x, ... \end{aligned} \tag{27}$$

ある従属変数 $f(t_0, t_1, t_2, x_0, x_1, x_2, ...)$ に対して, t と x に対する偏導関数は, slow variables を用いて, 以下のように展開される：

$$\begin{aligned} \frac{\partial f}{\partial t} &= \frac{\partial f}{\partial t_0} + \epsilon \frac{\partial f}{\partial t_1} + \epsilon^2 \frac{\partial f}{\partial t_2} + \cdots, \\ \frac{\partial f}{\partial x} &= \frac{\partial f}{\partial x_0} + \epsilon \frac{\partial f}{\partial x_1} + \epsilon^2 \frac{\partial f}{\partial x_2} + \cdots. \end{aligned} \tag{28}$$

3.2 線形方程式系 従属変数の摂動展開, パラメータのオーダー評価, また slow variables の定義などを, 基礎方程式系に代入し, ϵ の恒等式として整理してゆく.

まず, $O(\epsilon)$ の方程式系として, 以下を得る (順に, 気相および液相の質量保存則と運動量保存則, Keller の方程式を表す)：

$$\frac{\partial \alpha_1}{\partial t_0} - 3\frac{\partial R_1}{\partial t_0} + \frac{\partial u_{G1}}{\partial x_0} = 0, \tag{29}$$

$$-\alpha_0 \frac{\partial \alpha_1}{\partial t_0} + (1-\alpha_0)\frac{\partial u_{L1}}{\partial x_0} = 0, \tag{30}$$

$$\beta_1 \frac{\partial u_{G1}}{\partial t_0} - \beta_1 \frac{\partial u_{L1}}{\partial t_0} - 3\gamma \hat{p}_{G0} \frac{\partial R_1}{\partial x_0} = 0, \tag{31}$$

$$\begin{aligned} &-\alpha_0 \beta_1 \frac{\partial u_{G1}}{\partial t_0} + (1-\alpha_0+\beta_1\alpha_0)\frac{\partial u_{L1}}{\partial t_0} \\ &\qquad + (1-\alpha_0)\frac{\partial p_{L1}}{\partial x_0} = 0, \end{aligned} \tag{32}$$

$$\frac{\partial^2 R_1}{\partial t_0^2} + R_1 + \frac{p_{L1}}{\Delta^2} = 0. \tag{33}$$

方程式系 (29)-(33) は, R_1 を従属変数とする, 単一線形偏微分方程式

$$\begin{aligned} \mathcal{L}_1[R_1] \equiv &\frac{\partial^2 R_1}{\partial t_0^2} - \frac{\Delta^2}{3\alpha_0}\frac{\partial^4 R_1}{\partial x_0^2 \partial t_0^2} \\ &- \left[\frac{\Delta^2}{3\alpha_0} + \frac{(1-\alpha_0+\beta_1)\gamma\hat{p}_{G0}}{\beta_1(1-\alpha_0)}\right]\frac{\partial^2 R_1}{\partial x_0^2} = 0, \end{aligned} \tag{34}$$

にまとめられる. なお, 以後の表記のため, 線形演算子 $\mathcal{L}_1$ を導入した.

式 (34) の解を, 以下のように仮定する：

$$R_1 = A e^{i\theta} + c.c., \tag{35}$$

ここに, $A(t_1, x_1, t_2, x_2, ...)$ は slow variables に依存して時間および空間的にゆっくり変化する複素振幅である. なお, 記号 c.c. はその記号より左側にあるすべての複素数の複素共役を表し, i は虚数単位である. また, θ は位相関数であり

$$\theta \equiv k^* x_0^* - \omega^* t_0^* = k x_0 - \Omega t_0, \tag{36}$$

と表される (無次元波数 $k = k^* L^*$ を導入).

解 (35) を, 方程式系 (29)-(33) に代入し, t_0 や x_0 で積分して初期条件や無限遠方の境界条件を考慮すれば, 1 次の摂動項 α_1, u_{G1}, u_{L1}, p_{L1} を順次得る. それらはすべて, R_1 の定数倍で表される.

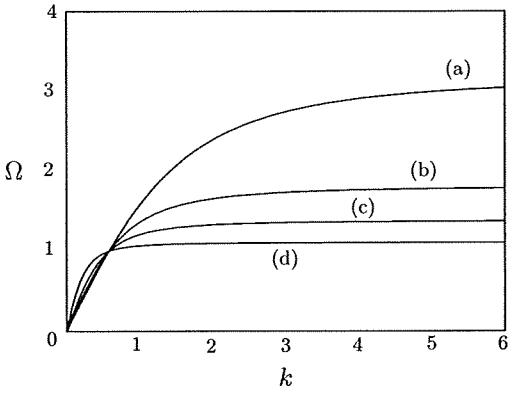

Fig. 2: Linear dispersion relation in the case of $\gamma = 1$, $\beta_1 = 1/2$ and $\hat{p}_{G0} = 1$: (a) $\alpha_0 = 10^{-2}$, $\Delta = 0.1$, (b) $\alpha_0 = 10^{-2}$, $\Delta = 0.2$, (c) $\alpha_0 = 10^{-3}$, $\Delta = 0.1$ and (d) $\alpha_0 = 10^{-3}$, $\Delta = 0.1$.

3.3 線形分散関係式と位相速度, 群速度 式 (34) に解 (35) を代入すれば, 線形分散関係式

$$\begin{aligned} D(k,\Omega) = &\frac{\Delta^2 k^2 (1-\Omega^2)}{3\alpha_0} \\ &+ \frac{(1-\alpha_0+\beta_1)\gamma\hat{p}_{G0}}{\beta_1(1-\alpha_0)}k^2 - \Omega^2 = 0, \end{aligned} \tag{37}$$

を得る. ここで, Δ と α_0 を適当に選び 4 通りの場合についての分散関係を, 図 2 に示す.

無次元位相速度 v_p, 無次元群速度 v_g を, それぞれ

$$v_p \equiv \frac{v_p^*}{U^*}, \quad v_g \equiv \frac{v_g^*}{U^*}, \tag{38}$$

と定義する. ここに, $v_p^* = \omega^*/k^*$ は位相速度, $v_g^* = \mathrm{d}\omega^*/\mathrm{d}k^*$ は群速度である. 無次元位相速度, 無次元群速度, また群速度の波数での 1 階微分は, それぞれ, 以下のように与えられる：

$$v_p = \frac{\Omega}{k}, \tag{39}$$

$$v_g = \frac{3\alpha_0\Omega}{k(3\alpha_0 + \Delta^2 k^2)}, \tag{40}$$

$$\frac{\mathrm{d}v_g}{\mathrm{d}k} = -\frac{9\alpha_0\Delta^2\Omega}{(3\alpha_0+\Delta^2k^2)^2}. \tag{41}$$

3.4 代表スケールの決定 代表的な周期の決定 (23) に続いて, 代表的な速度 U^* および長さ L^* を決定する. $\omega^* \equiv \omega_B^*$ (すなわち $\Omega \equiv 1$) と定めた上で, $v_g = 1$ を満足するような U^* と L^* を選ぶ. すなわち

$$L^* \equiv \frac{3\alpha_0}{k^*(3\alpha_0 + R_0^{*2}k^{*2})}, \quad U^* \equiv \frac{3\alpha_0\omega_B^*}{k^*(3\alpha_0 + R_0^{*2}k^{*2})}, \tag{42}$$

と定める. さらに, 群速度 v_g を 1 と定めたことから

$$\frac{3\alpha_0}{k(3\alpha_0+\Delta^2k^2)} = 1, \tag{43}$$

の関係を得る. 同時に, 式 (18) および (19) も満足する必要がある.

3.5　2 次の解析より得る遠方場の方程式　つづいて, $O(\epsilon^2)$ の方程式系を導出したのちに, 3.2 節とおなじく, R_2 を未知変数とする単一式にまとめる：

$$\mathcal{L}[R_2] = -\frac{1}{3}\frac{\partial N_1}{\partial t_0} - \frac{1}{3\alpha_0}\frac{\partial N_2}{\partial t_0} + \frac{1-\alpha_0+\beta_1}{3\beta_1(1-\alpha_0)}\frac{\partial N_3}{\partial x_0} + \frac{1}{3\alpha_0(1-\alpha_0)}\frac{\partial N_4}{\partial x_0} - \frac{\Delta^2}{3\alpha_0}\frac{\partial^2 N_5}{\partial x_0^2} \equiv H_2. \quad (44)$$

式 (44) の非同次項 H_2 は, R_1 や u_{G1} などの 1 次の摂動項から形成される. それらを代入し, 整理すれば

$$H_2 = \hat{C}A^2 e^{2i\theta} + i\left(-\frac{\partial D}{\partial \Omega}\right)\left(\frac{\partial A}{\partial t_1} + v_g\frac{\partial A}{\partial x_1} + CA\right)e^{i\theta} + c.c., \quad (45)$$

を得る (係数 $\hat{C}$ の陽な表現は複雑ゆえ省略).

H_2 には, $e^{i\theta}$ および $e^{-i\theta}$ に比例する項が含まれており, このままでは永年項が生じて漸近展開 (12)-(16) が一様に有効とはならない. よって, 永年項が現れないための条件 (可解条件)

$$\frac{\partial A}{\partial t_1} + v_g\frac{\partial A}{\partial x_1} + CA = 0, \quad C = \frac{V\Delta^3 k^2}{2(3\alpha_0 + \Delta^2 k^2)}, \quad (46)$$

を課す. 以後, 式 (46) を, t_1 に関する導関数と, x_1 に関する導関数を変換する際に使用する. 偏微分方程式 (46) の一般解, すなわち, 複素振幅 A の t_1 と x_1 に関する遠方場におけるふるまいは

$$A(t_1, x_1) = B(\varphi)\exp(-Ct_1), \quad (47)$$

にしたがう. ここに, B は移動座標 $\varphi = x_1 - v_g t_1$ のみに依存する任意関数である.

R_2 に関する偏微分方程式 (44) の解 (特解) は

$$R_2 = \frac{\hat{C}}{D(2k, 2\Omega)}A^2 e^{2i\theta} + c.c., \quad (48)$$

で与えられる. なお, 式 (44) の同次方程式の一般解は省略した.

つづいて, 解 (48) を, $O(\epsilon^2)$ の方程式系に代入することで, u_{G2}, u_{L2}, p_{L2}, α_2 も導くことができる.

3.6　散逸効果を含む非線形 Schrödinger 方程式　$O(\epsilon^3)$ の方程式系を導出し, 同様な操作を行う. すなわち, まず, $O(\epsilon^3)$ の 5 つの方程式から, α_3, u_{G3}, u_{L3}, p_{L3} を消去して, R_3 と $O(\epsilon^2)$ までの解析ですでに得られている低次の変数からなる単一の方程式を導出し, これを

$$\mathcal{L}[R_3] = H_3, \quad (49)$$

の形に表す. 次に, 式 (49) の可解条件にしたがって, 非同次項 H_3 の中に含まれる $e^{i\theta}$ に比例する項の係数をゼロとする.

その結果, 複素振幅 A の t_2 と x_2 に関する遠方場を記述する, 2 階非線形偏微分方程式

$$i\frac{\partial A}{\partial \tau} + \frac{1}{2}\frac{\mathrm{d}^2\Omega}{\mathrm{d}k^2}\frac{\partial^2 A}{\partial \xi^2} + \nu_1|A|^2 A + \nu_2 A = 0, \quad (50)$$

を得る. ここで, 非線形効果による補正を含む群速度で進む座標系への変数変換として

$$\tau = t_2, \quad \xi = x_1 - (v_g - i\epsilon\nu_3)t_1, \quad (51)$$

とおいた. 係数 ν_2 および ν_3 は, 音響放射減衰の効果に基づくものである. なお, 係数 ν_i $(i = 1, 2, 3)$ の具体的な形は, 本稿では省略する.

式 (50) が記述する, 包絡波の波形などの, 詳細は講演時に述べる.

4　おわりに

2 流体モデルに基づく, 気泡を含む圧縮性液体の運動を記述する方程式を起点として, $O(\epsilon^3)$ までの方程式に対する解析から, 式 (50) を得た. これは, 一般に強分散性媒質中における非線形波動の遠方場を記述する, 非線形 Schrödinger 方程式に, 音響放射減衰に起因する, 複素振幅の定数倍を付加したものとなっている.

今後, その解構造を把握してゆくこと, また弱分散性媒質に対する解析 [3] との比較を行うこと [9] が展望である.

謝辞

本研究は, 平成 20 年度厚生労働省科学研究費補助金 (医療機器開発推進研究事業：ナノメディシン研究 (H19-nano-010) によりなされたものである. ここに記して謝意を表す.

参考文献

[1] Egashira, R., Yano, T. and Fujikawa, S., "Linear wave propagation of fast and slow modes in mixtures of liquid and gas bubbles," *Fluid Dyn. Res.*, **34**, 317–334 (2004).

[2] Yano, T., Egashira, R. and Fujikawa, S., "Linear analysis of dispersive waves in bubbly flows based on averaged equations," *J. Phys. Soc. Jpn.*, **75**, 104401–01–08 (2006).

[3] 金川哲也, 矢野 猛, 渡部正夫, 藤川重雄, "殻付き微細気泡群を含む液体中における非線形波の伝播," 日本流体力学会年会 2008 (2008).

[4] Haga, T., Yano, T. and Fujikawa, S., "Propagation characteristics of linear pressure waves in water containing microbubbles," *Proc. 7th JSME-KSME Thermal and Fluids Engineering Conference*, Japan (2008).

[5] Whitham, G. B., *Linear and Nonlinear Waves*, (Wiley, New York, 1974).

[6] Eames, I. and Hunt, J. C. R., "Forces on bodies moving unsteadily in rapidly compressed flows," *J. Fluid Mech.*, **505**, 349–364 (2004).

[7] Keller, J. B. and Kolodner, I. I. "Damping of underwater explosion bubble oscillations," *J. Appl. Phys.*, **27**, 1152–1161 (1956).

[8] Jeffrey, A. and Kawahara, T., *Asymptotic Methods in Nonlinear Wave Theory*, (Pitman Advanced Pub. Program, Boston, 1982).

[9] Kanagawa, T., Yano, T., Watanabe, M. and Fujikawa, S., "Weakly nonlinear analysis of dispersive waves in mixtures of liquid and gas bubbles based on a two-fluid model," *Proc. 7th International Symposium on Cavitation*, America (2009) submitted.